This is a preprint, the final version is subject to change, of the American Mineralogist (MSA)
Cite as Authors (Year) Title. American Mineralogist, in press.
DOI: https://doi.org/10.2138/am-2019-6768

MS 6768; Revision 1

The incorporation of chlorine into calcium amphibole

David M. Jenkins[1]

[1] Department of Geological Sciences and Environmental Studies

Binghamton University

Binghamton, NY 13902

Running title: Chlorine in calcium amphiboles

Abstract

The exchange of halogens between fluids and solid silicates holds considerable potential to shed light on fluid-rock interactions associated with various geological processes, including seawater–ocean-crust interaction, crustal and mantle metasomatism, and economic deposit formation. This study reports on how variations in formation conditions (temperature, pressure, hydrogen fugacity), bulk composition (Na and K ratio), and choice of starting material salts affect the Cl contents of calcium amphiboles synthesized specifically from ferro-pargasite and hastingsite bulk compositions. Syntheses were attempted over the range of 600-950°C and 0.1-0.45 GPa at $\log f_{H2}$ of 1.4 to 2.4 (equivalent to -0.9 to -2.1 $\log f_{O2}$ below the fayalite-magnetite-β-quartz

Always consult and cite the final, published document. See http:/www.minsocam.org or GeoscienceWorld

oxygen buffer, or ΔFMβQ) for durations of 111-672 h. Amphiboles were characterized by powder X-ray diffraction and electron microprobe, with cation proportions calculated on the basis of an assumed 18% ferric iron content. Amphiboles formed from the ferro-chloro-pargasite bulk composition [$NaCa_2(Fe_{4.0}Al)(Al_2Si_6)O_{22}Cl_2$] had Cl contents of only about 0.5 atoms per formula unit (apfu), compared to the intended 2.0, and whose stabilities were about 70°C lower at 0.1-0.2 GPa than reported in a previous study of Cl-free (OH-bearing) ferro-pargasite. Syntheses on the ferro-pargasite bulk composition in the presence of a brine with a nominal mole fraction of Cl (X_{Cl}) of 0.3 over the range of 700 – 950°C at 0.2 GPa showed that temperature had less effect on the Cl content of the amphibole than small variations in the brine concentration assessed after treatment. For the chloro-hastingsite bulk composition [$NaCa_2(Fe_{4.0}Fe^{3+})(Al_2Si_6)O_{22}Cl_2$] , the Cl content of the product amphibole was unaffected by the specific choice of chloride salt or salt combinations (NaCl, $CaCl_2$, $FeCl_2$), but showed a direct correlation with the substitution of K for Na. Experiments done over the range of 0.10-0.45 GPa at 700°C and at -1.3 logf_{O2} ΔFMβQ showed an increased rate of nucleation of amphibole with increasing pressure for a hastingsite bulk composition with 40% substitution of K for Na, but no variation in the Cl content of the amphibole. Classification of the amphiboles formed in this study showed that a number of them were well outside their intended field, with some of those formed from the ferro-pargasite bulk composition straddling the boundary between hastingsite and ferro-pargasite, while a number of those formed from the hastingsite bulk composition were actually ferro-ferri-hornblendes. These results confirm that K more so than Na is important for the incorporation of Cl into calcium amphiboles, and that Cl-bearing ferro-ferri-hornblende, with low A-site Na + K, can form even from mixtures with abundant Na + K. Combining these observations with the strong correlation between Cl content and Fe# [=

Always consult and cite the final, published document. See http:/www.minsocam.org or GeoscienceWorld

45 $Fe^{2+}/(Fe^{2+} + Mg)$] noted in previous studies, a general correlation was found to exist between the
46 Cl content and the FeAlK index, defined as Fe#·(^{T}Al + K), which combines the effects of Fe#,
47 tetrahedrally-coordinated Al (^{T}Al), and K content. A linear trend is observed once a minimum
48 value of about 0.34 in the FeAlK index is reached. The implication is that the crystal-chemical
49 controls for Cl incorporation in calcium amphiboles are dominated by substitution of Fe^{2+} for
50 Mg, ^{T}Al for Si, and K for Na into the crystallographic A site with a linear dependence at the rate
51 of 0.45 Cl per FeAlK index above a minimum value of about 0.34.

52 Keywords: Ferro-pargasite, hastingsite, chlorine, chloro-amphibole, synthesis, ferro-ferri-
53 hornblende

54 **Introduction**

55 In contrast to a relatively rich history of experimental studies on F-bearing amphibole
56 synthesis and stability (e.g., Bowen and Schairer, 1935; Comeforo and Kohn, 1954; Gilbert et
57 al., 1982; Robert et al., 1989; Raudsepp et al., 1991; Jenkins and Hawthorne, 1995; Pavlovich
58 and Jenkins, 2003), there are few experimental studies on the incorporation of Cl into
59 amphiboles. With a growing interest in the use of halogens to monitor geological processes
60 ranging from seawater–ocean-crust interactions (e.g., Barnes and Cisneros, 2012; Kendrick et al.,
61 2015) and crustal shear-zone metasomatism (Kusebauch et al., 2015) to mantle metasomatism
62 (Frezzotti et al., 2010; Selverstone and Sharp, 2011) and the formation of economic deposits
63 (Yardley and Bodnar, 2014), there is a need to understand the compositional variations that
64 permit uptake of Cl by amphibole. To be sure, establishing these crystal-chemical controls is
65 only one side of the broader issue concerning the partitioning of Cl into amphibole, the other
66 being the response of the amphibole to variations in the activity of Cl in the ambient brine or
67 melt. Although some research has been reported on the effect of variable chloride-brine

Always consult and cite the final, published document. See http:/www.minsocam.org or GeoscienceWorld

concentrations (Chan et al., 2016; Campanaro and Jenkins, 2017), the present study focuses on the first issue by considering either what crystal-chemical controls are exerted by the amphibole, or what chemical changes occur in concert with the incorporation of Cl into amphibole.

Two amphiboles that are commonly found to contain elevated Cl contents are ferro-pargasite [$NaCa_2(Fe^{2+}{}_4Al)(Al_2Si_6)O_{22}(OH)_2$] and hastingsite [$NaCa_2(Fe^{2+}{}_4Fe^{3+})(Al_2Si_6)O_{22}(OH)_2$] (e.g., Makino et al., 1993; Mazdab, 2003; McCubbin et al., 2013; Giesting and Filliberto, 2016). These two amphiboles, differing only in the proportion of Al^{3+} versus Fe^{3+} in the octahedrally-coordinated *M*(2) site, can occur individually or together. Ferro-pargasite occurs in a broad range of igneous (diorite, nepheline syenite) and metamorphic (garnet granulite, eclogite, amphibolite, and metamorphosed carbonates, Deer et al., 1997, Table 14) lithologies, while hastingsite occurs in acid and alkaline plutonic rocks (Deer et al., 1997, p. 434). Occasionally they occur together, such as in an alkaline feldspar syenite in the Chhotaudepur area of India (Hari et al., 2014) or alkali-feldspar granites of the Carajás metallogenic province, Brazil (Barros et al., 2009). Outside of the general conditions attending the formation of hastingsite and ferro-pargasite, there is no clear consensus on the conditions needed to form Cl-rich ferro-pargasite or hastingsite. Giesting and Filiberto (2016) provided a review of the limited number of terrestrial occurrences where chloro-amphiboles occur, that is, those having Cl apfu (atoms per formula unit) in excess of OH + F. The conditions reported in the literature range from low-temperature ($\geq$ 350°C) halogen-rich fluids in the Fraser Mine, Sudbury, Ontario, Canada (McCormick and McDonald,1999) to high-temperature (600-700°C) metasomatic fluids in the Bamble sector, S.E. Norway (Kusebauch et al., 2015). Deducing the formation conditions in field localities with chloro-amphiboles is complicated by the frequent presence of multiple metamorphic overprints, multiple episodes of fluid-rock interactions, and the likely presence of an evolving fluid

Always consult and cite the final, published document. See http:/www.minsocam.org or GeoscienceWorld

composition yielding successively higher Cl contents when there is limited fluid interaction with the host rock (e.g., Kusebauch et al., 2015; Rebay et al., 2015). In contrast, an experimental investigation can control some of these variables and help shed new light on the origin of Cl-rich amphiboles.

This study summarizes experimental work concerning what effects certain variations in the starting-material bulk compositions and synthesis conditions have on the incorporation of Cl into amphiboles synthesized from ferro-pargasite and hastingsite bulk compositions.

Methods

Apparatus

Syntheses were done in two types of apparatus. The first type of vessel, used for most of the experiments at 0.2 GPa, was externally-heated cold-seal vessels, constructed of René 41 (a Ni-rich alloy). The pressure medium was water; however, a short length of iron rod (~1 cm long by 0.3 cm diameter) was placed next to the capsule to reduce the oxygen fugacity (f_{O2}) by reaction with the pressure-medium water. This filler-rod method was used for creating a reducing environment instead of the double-capsule method (e.g., Chou, 1987) to permit long-duration experiments (200-500 h) to be done without risk of expending the buffer in a double-capsule configuration and to permit larger volumes of material to be made in a given experiment. This method generally does not produce an oxygen fugacity defined by a particular buffering assemblage, but instead was used simply to establish a reducing environment that was broadly compatible with the stability field of the amphiboles investigated in this study. Inspite of the various issues surrounding this method, such as diffusion of H_2 through high-temperature vessel walls or armoring of the reactive filler-rod material (magnetite/wüstite over iron in this case), it has been shown by Matthews et al. (2003) that steady-state hydrogen fugacities (f_{H2}) can be

Always consult and cite the final, published document. See http:/www.minsocam.org or GeoscienceWorld

reached in Ni-rich pressure vessels within about 20 hours that are stable for durations up to 800 h. As discussed in Chan et al. (2016), the oxygen fugacity imposed on the sample in this configuration was determined, using separate sensor capsules containing mixtures of Co and CoO or magnetite and wüstite as well as the CoO-MnO-Co variable oxygen sensor of Pownceby and O'Neill (2000), to have log(f_{O2}) values between -18.1 and -17.7 at 0.2 GPa and 700°C, which is within the f_{O2} ranges defined by the Co-CoO and magnetite-wüstite buffers.

The second apparatus was internally-heated gas vessels of the type described by Holloway and Wood (1988) using hydrogen-argon gas mixtures as the pressure medium and nichrome wound furnaces. It was found that nichrome (80% Ni) was less susceptible to hydrogen embrittlement and failure than Fe-based heating elements (e.g., Kanthal A-1®). A reducing environment inside the vessel was produced by first introducing hydrogen gas at a given pressure, shutting off the hydrogen gas supply, and then pressurizing the vessel with argon to attain a desired total pressure in a H_2-Ar mixture at room temperature. At this point both gas supplies were closed off which established the partial pressure of H_2 and, therefore, mole fraction of H_2 (X_{H2}) in the gas mixture. The final pressure was attained through thermal expansion of the gas and the fugacity of H_2 was calculated at the final pressure and temperature (P-T) by multiplying the fugacity coefficient for H_2 (γ_{H2}, Shaw and Wones, 1964) at the corresponding P-T conditions to the mole fraction of H_2 in the gas, i.e., $f_{H2} = P \cdot X_{H2} \cdot \gamma_{H2}$. Figure 1a is a comparison of the calculated f_{O2} (based on the imposed f_{H2}) as a function of the observed f_{O2} measured by the sensor method of Pownceby and O'Neill (2000) for a selection of internally-heated gas-vessel experiments. There is relatively good agreement, although the observed f_{O2} tends to be shifted lower than the intended (calculated) value, particularly at conditions near the upper-limit of this sensor (Co-CoO buffer, grey circle). Individual data points are labeled with

Always consult and cite the final, published document. See http:/www.minsocam.org or GeoscienceWorld

the duration of the experiment showing that there is no obvious correlation in the observed oxygen fugacity with the length of treatment time that might arise from changes in oxidation state related, for example, to diffusive loss of hydrogen from the pressure vessel. Temperatures were measured using two Inconel®-sheathed chromel-alumel thermocouples whose hot-junction tips straddled the sample position, such that the stated uncertainties in temperature included both the precision of temperature measurement (± 2°C) and any thermal gradient across the sample capsule.

Starting materials

All syntheses were made using mixtures of reagent-grade oxides, carbonates, metallic iron, and chlorides. The reagents were SiO_2, which was made by desiccating silicic acid by step-wise heating to 1100 °C overnight, Al_2O_3, Fe_2O_3, $CaCO_3$, Na_2CO_3, K_2CO_3, metallic Fe (~10 μm grain size), NaCl, $CaCl_2$, and "$FeCl_2$". The NaCl was dried for 24 hours in air at 580°C to remove water trapped in aqueous fluid inclusions present in the salt (as received) by thermal decrepitation of the inclusions. For most of the syntheses done in this study $FeCl_2$ was used as the source of Cl ion. The "$FeCl_2$" as received was determined by X-ray powder diffraction (XRD) and Rietveld refinement to be a mixture of 40 mol% $FeCl_2$ and 60 mol% $FeCl_2 \cdot 2H_2O$; adjustments were made for this additional water of hydration during the weighing of this reagent. It was further found by *in situ* heating in a powder diffractometer that single-phase $FeCl_2$ is obtained by heating "$FeCl_2$" to 160°C for 15 min in air. Therefore, all treatments of starting mixtures involving "$FeCl_2$" were heated to 160°C for 15 min prior to being sealed in capsules, as described below. Careful handling of the $CaCl_2$ was exercised to account for its hygroscopic nature. Mixtures including $CaCl_2$ were prepared by weighing the approximate amount of $CaCl_2$ into a pre-weighed flask, fitted loosely with a fritted-glass stopper, dried to 200°C for 30 min to

Always consult and cite the final, published document. See http:/www.minsocam.org or GeoscienceWorld

thoroughly desiccate the $CaCl_2$ (confirmed by XRD with *in situ* heating) but prevent oxidation to CaO, firmly inserting the stopper, cooling, and then obtaining the final weight of the $CaCl_2$.

Starting mixtures were prepared as follows. The SiO_2, Al_2O_3, and any carbonates ($CaCO_3$, Na_2CO_3, and/or K_2CO_3) were weighed and mixed together under acetone until dry. This mixture was then heated in air at 900°C for 15 min, which has been found to be sufficient time to decarbonate the mixture by reaction with SiO_2 but purposely kept short to minimize volatilization of Na or K from the mixture. To this decarbonated mixture was added Fe_2O_3 and metallic Fe in proportions equivalent to FeO, any extra Fe2O3 if needed, and the chloride source ("$FeCl_2$", $CaCl_2$, and/or NaCl), which were all mixed together dry to avoid any separation of reagents by density differences or dissolution of the highly soluble "$FeCl_2$" by any organic solvent. The list of bulk compositions investigated in this study is given in Table 1.

Sample treatment

Portions of the starting mixtures were encapsulated in $Ag_{50}Pd_{50}$ alloy capsules made from tubing that was either 3.0 or 1.5 mm outer-diameter by 0.13 mm wall thickness. Mixtures that used "$FeCl_2$" as the chloride source were heated at 160°C for 15 min in air, crimped while still hot (to minimize subsequent exposure to air), and then sealed by arc welding under a lightly moistened tissue to help mask the AgPd-melt from exposure to oxygen (Weidner, 1989). Mixtures with $CaCl_2$ were heated to 200°C for 15-30 min, crimped, and sealed in the same manner as for the "$FeCl_2$"-bearing mixtures.

In this laboratory it was found that the use of $Ag_{50}Pd_{50}$ alloy not only minimizes Fe uptake from the sample (Driscall et al., 2005) but also increases the amphibole yield at a given set of *P*-*T*-f_{O2} conditions. A series of syntheses were made using the ferro-chloro-pargasite composition (FEPG 1) in Table 1 and all done at 600°C and 0.2 GPa for 13-19 days in cold-seal vessels but

Always consult and cite the final, published document. See http:/www.minsocam.org or GeoscienceWorld

using four different capsule materials: $Ag_{50}Pd_{50}$, $Ag_{70}Pd_{30}$, Pt, and Au. Only the $Ag_{50}Pd_{50}$ alloy produced a strong (58 wt%) amphibole yield (with coexisting plagioclase, fayalite, and salts), while the other capsule materials produced either little amphibole (18 wt%, $Ag_{70}Pd_{30}$) or no amphibole (Au, Pt). The presence of magnetite and quartz in syntheses with little or no amphibole yields compared with fayalite in the high-amphibole yields suggests that a more reduced environment (below the fayalite-magnetite-β-quartz, FMβQ, oxygen buffer) is more favorable for amphibole growth. Setting aside the synthesis done in the Pt capsule, where alloying of iron oxide with the capsule may create an oxidizing environment that is not conducive to amphibole formation, there appears to be a correlation in amphibole yield with increasing permeability of the capsule material to hydrogen ($Au << Ag_{70}Pd_{30} < Ag_{50}Pd_{50}$). It may be that the increased permeability of Pd-rich capsules to hydrogen, as can be seen even going from $Ag_{80}Pd_{20}$ to $Ag_{70}Pd_{30}$ (Chou, 1986), might provide an initially more reduced environment that expedites formation of amphibole. Whether it is hydrogen permeability or some other factor (e.g., surface catalysis),this reconnaissance study supports the choice of $Ag_{50}Pd_{50}$ as the preferred capsule material for this study.

Analytical methods

Powder X-ray diffraction (XRD) patterns of the synthesis products were obtained on a Panalytical PW3040-MPD X-ray diffractometer operated at 40 kV and 20 mA using Cu K_α radiation with a graphite diffracted-beam monochromator. Samples were mounted on a zero-background quartz plate and scanned from 5-60° 2Θ using step sizes of 0.04° 2Θ and measured for durations sufficient for obtaining ~1000 counts on the strongest peaks. Rietveld refinements were made using the General Structure Analysis System (GSAS) software of Larson and Von Dreele (2004).

Always consult and cite the final, published document. See http:/www.minsocam.org or GeoscienceWorld

Electron microprobe analysis was done on a JEOL 8900 Superprobe using samples mounted in epoxy and polished with diamond abrasive in successively finer grits to a final size of 0.5 μm. The operating conditions for all analyses were 15 kV and 10 nA using albite as the standard for Na, wollastonite for Ca, the pure oxides for Fe, Al, and Si, orthoclase for K, and reagent $PdCl_2$ for Cl. Matrix corrections were made with the ZAF scheme. Chlorine X-ray counts were monitored for the $PdCl_2$ standard and both sodium and chlorine X-ray counts were monitored for amphiboles from sample RW-S1 of Johnson et al. (2004) containing about 1.3 wt% Cl and 1.4 wt% Na_2O to determine the extent of Na and Cl diffusion under the electron beam. There was no discernible loss of counts over counting durations of 1-2 minutes in spot mode (~ 1 μm diameter) for either the Cl standard or amphibole. Even so, the counting times for WDS analyses of the major elements (Na, Mg, Al, Si, Ca, K, and Fe) were kept to 10 s on the peak and 3 s on the background to minimize Na diffusion from the standards and the samples. Because of the relatively low Cl contents observed for many of the amphiboles, Cl was measured using 30 s on the peak and 10 s on the background. It should be noted that analysis of fine-grained minerals, such as the amphiboles formed in this study, often results in the X-ray excitation volume exceeding the volume of the grain and resulting in low analytical totals. This situation has been studied in considerable detail in this lab (e.g., Giblin et al., 1993; Jenkins and Corona, 2006) where it has been shown that analyses with analytical totals even as low as 65-70 wt% give stoichiometries that are essentially equivalent to coarse-grained minerals. In this study, most analyses were well above this minimum, typically in the range of 80-98 wt%.

Cations in the amphibole structure ($AB_2C_5T_8O_{22}W_2$) were calculated initially assuming all iron was ferrous and adding sufficient OH to have the sum of OH+Cl in the W sites equal 2.0. In many cases this did not result in a feasible amphibole formula (e.g., cation sums above 16.0), in

Always consult and cite the final, published document. See http:/www.minsocam.org or GeoscienceWorld

which case ferric iron was introduced under the assumption that the ferric-iron proportion (= $Fe^{3+}/\sum Fe$) was a constant value of 18%. This value is based on the studies of Chan et al. (2016) and Mueller et al. (2017) where amphiboles were synthesized from the bulk compositions ferro-pargasite and those made along the magnesio-hastingsite–hastingsite [$NaCa_2(Mg_4Fe^{3+})(Al_2Si_6)O_{22}(OH)_2$- $NaCa_2(Fe_4Fe^{3+})(Al_2Si_6)O_{22}(OH)_2$] join , respectively, using the same methods and techniques used in this study and for which selected amphiboles were analyzed by Mössbauer spectroscopy. Further discussion for the choice of 18% ferric iron can be found in Campanaro and Jenkins (2017); nevertheless, the effect on the classification of amphiboles made in this study by varying the percentage of ferric iron over the full 2σ range (± 6%) reported by Campanaro and Jenkins (2017) is discussed below. Cations for ferric-oxide-corrected microprobe analyses were then determined by having the sum of O+OH+Cl = 24 and either adding sufficient OH to have the sum of OH+Cl in the W sites equal 2.0, or sufficient OH to have the sum of T- and C-site cations (excluding Ca, Na, and K) equal 13. The latter method allows for the presence of oxo-amphibole component and the attendant deficit of OH, which, if one forces the W sites to sum to 2.0, can yield a deficiency of C-site cations. Cations were distributed in a conventional manner, namely filling the T sites first with Si then Al to sum to 8, assigning the remaining Al, Fe^{3+}, and sufficient Fe^{2+} (in that order) to the C sites to sum to 5, putting excess Fe^{2+} into the B sites along with sufficient Ca and Na to sum to 2, and assigning any remaining Ca, Na, and K to the A sites. Resultant mineral formulae with cation totals below 15.0 or above 16.05 were rejected.

Results

Ferro-pargasite bulk composition

Hydrogen fugacity (f_{H2})

Always consult and cite the final, published document. See http:/www.minsocam.org or GeoscienceWorld

The study of Gilbert (1966) determined temperatures along a variety of oxygen-fugacity buffers where ferro-pargasitic amphibole is stable, which serves as a good frame of reference for understanding the dependence on hydrogen fugacity (f_{H2}) of the Cl-bearing ferro-pargasitic amphiboles formed in this study. Gilbert (1966) used the double-capsule approach for buffering the oxygen fugacity in water-rich experiments; however, in the present study the hydrogen fugacity was controlled directly and water was generally absent, or nearly so, in many of the syntheses. Therefore, the oxygen fugacities reported originally by Gilbert (1966) have been translated to the equivalent hydrogen fugacity (f_{H2}) using the oxygen-fugacity equations summarized by Frost (1991) and the thermodynamic properties of water at elevated pressures and temperatures of Holland and Powell (1990). The resultant $\log f_{H2}$-T curve for OH-ferro-pargasite is shown by the dashed curve in Figure 1b. Selected syntheses made from the bulk composition ferro-chloro-pargasite (FEPG 1, Table 1) are also shown in Figure 1b, where the solid circles represent amphibole growth, open circles no growth, and the half-shaded symbol gave mixed results as discussed in more detail in the next section. The approximate stability field for Cl-bearing ferro-pargasite from this study is shown by the solid curve, which is modeled after the curve of Gilbert (1966) but shifted about 70°C lower. In general, amphibole formed from the ferro-chloro-pargasite bulk composition has about 0.5 Cl apfu and has a lower thermal stability than OH-bearing ferro-pargasitic amphiboles at 0.1-0.2 GPa. A more detailed study of the effect of Cl on the thermal stability of ferro-pargasitic amphibole involving reaction reversal experiments is in progress, the preliminary results of which can be found in Jenkins (2018); the synthesis, as compared to the reaction reversal, experiments involving Cl-bearing ferro-pargasitic amphibole are shown here to demonstrate that they have the same general dependence on the fugacity of hydrogen (and, by extension, fugacity of oxygen) as OH-bearing ferro-pargasite.

Always consult and cite the final, published document. See http:/www.minsocam.org or GeoscienceWorld

Chloride brine concentration and temperature

A series of syntheses was done at 700°C and 0.2 GPa using ferro-pargasite bulk composition to which 10 wt% of different $FeCl_2$ brines were added (*Variable brine conc.*, Table 2). The results of these syntheses are shown in Figure 2, along with the synthesis of ferro-chloro-pargasite with only absorbed moisture (FEPG 1-2, Table 2). As can be seen in Figure 2 the results were variable. The lack of amphibole (open circles) for the lowest brine concentrations (0 – 0.036 X_{FeCl2}) contrasts sharply with the consistent growth of ferro-pargasitic amphibole treated in the presence of variable NaCl brines at 700°C and 0.2 GPa observed by Chan et al. (2016). The reason for the difference between this study and that of Chan et al. (2016) is unclear but may be related to the oxidation state that develops during treatment in a given brine. In the presence of pure water, with no added brine, a long-duration treatment (FEPG 3-16, 481 h) produced no amphibole. A second treatment (FEPG 3-17, Table 2) without any brine was purposely kept shorter (146 h) and yielded strong amphibole growth (square, Fig. 2). This shorter treatment time is more in line with the relatively short durations (~72 h) used in Chan et al. (2016) at low NaCl-brine concentrations, suggesting that there may be a gradual change from a more reducing to a more oxidizing environment inside the capsule with time in the presence of dilute brines that eventually destabilizes the amphibole. This is supported by the presence of magnetite in all of the amphibole-absent syntheses. Amphibole did form in $FeCl_2$ brines between 0.05 and about 0.3 $X_{FeCl_2}^{brine}$, suggesting that $FeCl_2$ brines in this concentration range were able to maintain a more reducing condition for longer durations (363 – 408 h) that stabilized amphibole, as supported by the presence of coexisting fayalite. The lack of amphibole at the highest $FeCl_2$ brine concentration is attributed at this time to both the reduced stability of Cl-rich ferro-pargasite at these *P-T* conditions and to a lower activity of H_2O in an $FeCl_2$ brine compared

Always consult and cite the final, published document. See http:/www.minsocam.org or GeoscienceWorld

298 to NaCl (cf, FEPG 3-5, Table 2) preventing the formation of an OH-bearing amphibole. Overall,
299 the variable results at these conditions (half-shaded symbol, Fig. 1b) may simply mean that
300 amphibole formation is very dependent on small differences in oxygen or water fugacity, relating
301 to the type of brine being used, for a given synthesis duration.

302 A series of syntheses on ferro-pargasite bulk composition was done at 0.2 GPa and 700-
303 950°C in the presence of 10 wt% of a NaCl brine with the *nominal* composition of $X_{\mathrm{NaCl}}^{\mathrm{brine}} = 0.3$.
304 These results are given in Table 2 (*Amphibole formation with T*) and shown in Figure 3a where
305 the Cl content of the amphibole, as determined from microprobe analysis of individual
306 amphibole grains (Table 3), is plotted as a function of the synthesis temperature. The lower
307 temperature syntheses might suggest a trend of decreasing Cl content with increasing
308 temperature, but taking all of the data together shows there is essentially no correlation (r =
309 0.058). These same data were replotted in Figure 3b to show the Cl content as a function of the
310 brine concentration determined after the treatment, where a more accurate assessment of the
311 water content in the capsule (generally the most challenging aspect of encapsulating a solid-
312 water mixture) could be made by puncturing, drying, and reweighing the encapsulated sample. It
313 can be seen in Figure 3b that there is an excellent correlation between the NaCl brine
314 concentration and the Cl content (r = 0.922), indicating that it is the brine concentration, rather
315 than temperature, that has the greater effect on the Cl content of amphibole.

316 **Hastingsite bulk composition**

317 Chloride salt type

318 In the earlier study by Chan et al. (2016) it was noted that $FeCl_2$ brines produced amphiboles
319 with higher Cl contents than NaCl brines. It was not clear at that time whether this was the result
320 of a higher Cl activity in the 1:2 $FeCl_2$ brine or was caused by some other aspect of the salt, such

Always consult and cite the final, published document. See http:/www.minsocam.org or GeoscienceWorld

as a stronger partitioning of Cl into the amphibole compared to the brine for $FeCl_2$ versus NaCl. This question is explored in a little greater detail here using the hastingsite bulk composition, which was observed by Mueller et al. (2017) to have higher Cl contents than ferro-pargasite and, therefore, is better suited for determining what controls the Cl content in the amphibole.

A series of syntheses were made on the bulk composition of chloro-hastingsite but using different chlorides ($CaCl_2$, $FeCl_2$) or combinations of chlorides (NaCl + ½ CaCl2, NaCl + ½ $FeCl_2$) in the starting mixtures, so that in each case there were 2 Cl apfu. Table 1 lists the four mixtures investigated here (HAST 12, 13, 14, 15), which were all run together in a single experiment. Each was treated as an anhydrous mixture, with particular care used to minimize incidental hydration during the capsule loading and sealing. The results are given in Table 2 (*Variable chloride salts in hastingsite*) and shown in Figure 4. Amphibole formed in each synthesis and the syntheses were effectively anhydrous, with no $X_{\mathrm{Cl}}^{\mathrm{brine}}$ below 0.95. Microprobe analyses (Table 3) indicate a very consistent Cl content, with the average being 0.76 ± 0.12 (1σ). These results indicate that, for anhydrous syntheses, the type of salt used is unimportant so long as the total Cl content is the same. Whether or not this independence of salt type continues down to more dilute brines remains to be determined, but at least for the extreme case of no dilution, there does not appear to be any discernable difference in salt type.

Effect of potassium

Amphiboles were synthesized from a series of bulk compositions with increasing substitution of K for Na in hastingstie at 700 °C, 0.34-0.46 GPa, and at $\Delta\log(f_{O2})$ FMβQ of about -1.3 for durations of 111-263 h (*K-Na substitution in hastingsite*, Table 2). Amphibole yields were quite good across this join, with one sample (HAST 6-2) producing only amphibole. These high yields are attributed, in part, to the choice of bulk compositions used for all of these mixtures

Always consult and cite the final, published document. See http:/www.minsocam.org or GeoscienceWorld

except one (HAST 10, Table 1) where the Ca content was purposely shifted to a slightly lower content of 1.8 apfu. This shift is consistent with the improved yields observed in previous studies of pargasitic (Sharma and Jenkins, 1999) and hastingsitic (Mueller et al., 2017) amphiboles. Electron microprobe analyses of these samples are listed in Table 3 and Figure 5a shows the observed Cl content as a function of the K content. A linear regression (diagonal line) to all of the data gives a reasonably high correlation coefficient (r = 0.836). Plotting the Cl contents of these same amphiboles as a function of the $FeCl_2$ brine concentrations in which they were synthesized (Table 2) gives a relatively poor correlation. This stands in contrast to the strong correlation observed for pargasitic amphibole (Fig. 3b). The strong correlation between Cl and K content observed here for hastingsitic amphibole is sometimes unclear for natural amphiboles, as discussed below.

Effect of pressure

To examine the effect of pressure, amphiboles were synthesized from the bulk composition HAST 7 in Table 1, all at 700°C and $\Delta\log(f_{O2})$ of about -1.3 relative to FMβQ, over the pressure range of 0.1 – 0.46 GPa. The results are listed in Table 2 (*Amphibole formation with P*). Rietveld refinements were done on these synthesis products with the specific purpose of estimating the weight percentages of the phases formed. Figure 6a shows an excellent correlation between the pressure of formation and the amphibole yield. The uncertainty (precision) in the weight% of amphibole derived during the Rietveld refinement is about the size of the symbol in this figure; however, the true uncertainties, as determined using calibration mixtures of silicates (e.g., Liogys and Jenkins, 2000), is probably closer to ± 2 or 3 wt%. The reason for increased amphibole yields with increasing pressure is uncertain but may be related to minor increases in Na + K for samples HAST 7-4 through HAST 7-7 in Table 3. This is

Always consult and cite the final, published document. See http:/www.minsocam.org or GeoscienceWorld

supported by the work of Mandler and Grove (2016) who noted a strong positive correlation between Na + K and pressure in amphiboles formed in ultramafic bulk compositions. It may also be that hastingsite, being stable at high pressures (Thomas, 1982), is more readily nucleated moving further inside the amphibole stability field. Figure 6b demonstrates that even though the proportion of amphibole increases with pressure the chlorine content of the amphibole that forms is essentially constant.

Discussion

Synthetic amphibole classifications

As is often the case for synthetic amphiboles, the observed amphibole composition is often shifted from the intended, or nominal, composition represented by the bulk composition of the starting mixture because of crystal-chemical and/or thermodynamic reasons. For example, this behavior has been seen for the simplest calcium amphibole tremolite, as summarized by Evans (2007), for the sodium amphibole glaucophane (Tropper et al., 2000, Jenkins and Corona, 2007), and for amphiboles along the tremolite-pargasite (Sharma and Jenkins, 1999) and tremolite-glaucophane (Jenkins, et al., 2013) joins. This is also the case in this study, where the amphiboles that are formed are generally removed from their intended compositions, often shifting them into a different classification for calcium amphiboles as defined by the latest IMA nomenclature scheme (Hawthorne et al., 2012). Figures 7a,b show the compositions of the amphiboles reported in Table 3 on a diagram that applies to the ^{W}(OH,F,Cl)-dominant amphibole group and that is designed to differentiate the calcium amphiboles investigated in this study based on their A-site occupancy of Na + K and C-site ratio of $Fe^{3+}/(Fe^{3+} + Al)$. It should be emphasized that the ferric iron content is estimated as 18% of the total iron content, as mentioned previously. To explore further the effect of this assumption on the classification of

Always consult and cite the final, published document. See http:/www.minsocam.org or GeoscienceWorld

amphiboles, the ferric iron content was allowed to vary by ± 6%, namely from 12 – 24% of the total iron content, and the cations recalculated as described in the methods section. Because the cations are calculated by adjusting the OH content at a given (fixed) ferric-iron content, rather than adjusting the ferric/ferrous iron ratio for an OH content that is fixed by stipulating that (OH+F+Cl) = 2 apfu or that (OH+F+Cl) = 2 – 2Ti as is commonly done (e.g., Hawthorne et al., 2012), the main result is that the ratio of $Fe^{3+}/(Fe^{3+} + Al)$ typically varies more so than the total A-site Na and K content. This variation is about 0.2 in the $Fe^{3+}/(Fe^{3+} + Al)$ ratio and from 0 up to 0.2 in the Na+K content, which is essentially the size of the (1σ) uncertainty bars shown in Figures 7a,b. Therefore, amphiboles that plot near a vertical boundary in Figures 7a,b may move from a more oxidized to more reduced field (e.g., ferro-ferri-hornblende to ferro-hornblende) but not necessarily into a more A-site rich field (e.g., ferro-ferri-hornblende to hastingsite).

Figure 7a shows the series of amphiboles (open circles) made from the ferro-pargasite bulk composition (FEPG 3, solid circle) over the temperature range of 700 to 900°C. Even though the trend is not monotonic, there is a general shift to lower $Fe^{3+}/(Fe^{3+} + Al)$ with increasing temperature (*T*) owing mostly to increasing ^{C}Al content and a concomitant shift towards ideal ferro-pargasite. The series of hastingsitic amphiboles formed from different chloride salts and salt combinations (open squares) lie well inside the hastingsite field, while the amphiboles formed from the potassic-hastingsite composition with 0.4 K apfu at variable pressure (grey squares) are all deficient in the total Na and K contents and plot inside the ferro-ferri-hornblende field. This is consistent with the trend observed in Figure 7b across the series of K-for-Na substituted hastingsite where the lowest K-contented amphiboles lie inside the ferro-ferri-hornblende field but move into the (potassic) hastingsite field with increasing K content. All of the observed amphibole compositions formed from hastingsite starting compositions (solid

Always consult and cite the final, published document. See http:/www.minsocam.org or GeoscienceWorld

413 squares) are depleted in ferric iron, enriched in octahedral Al, and depleted in A-site cations
414 shifting them towards, or even into, the pargasite and hornblende fields.

415 **Potassium – chlorine association**

416 At present there is some uncertainty as to whether or not potassium is correlated with
417 chlorine in calcium amphiboles. Previous studies have shown positive correlations between the
418 sum of Na and K at the A site and the Cl content (e.g., Morrison, 1991; Enami et al., 1992).
419 Some studies have identified a clear correlation between K and Cl, such as in the amphiboles of
420 the sheared gabbros in Lofoten, Norway (Kullerud, 1996), Dana Hill metagabbro of the
421 Adirondack Mountains, New York (Johnson et al., 2004), or the granulite-facies iron formations
422 of the eastern Beartooth Mountains, Montana (Henry and Daigle, 2018). In other studies,
423 however, the correlation between K and Cl is either conflicting, as in the altered eclogites of
424 Yangkou UHP complex in the Sulu UHP belt, northern China (Liu et al., 2009), or simply
425 unclear as in the Cl-bearing secondary hornblendes occurring in garnet peridotites of Cima di
426 Gagnone in the Lepontine Alps, Switzerland (Kendrick et al., 2018). The presence of K-rich
427 amphiboles with little or no detectable Cl (e.g., Mazdab, 2003; Banno et al., 2009; Pagano et al.,
428 2016) confirms that K does not necessarily enter amphibole as a coupled substitution with Cl.
429 However, synthesis of amphiboles from mixtures of hastingsite bulk composition that are
430 identical other than for the substitution of K for Na and are made under the same conditions
431 clearly demonstrates the positive correlation between K and Cl content (Fig. 5a).

432 **Pressure of synthesis**

433 Despite the increased yield of amphibole with increasing pressure (Fig. 6a), pressure appears
434 to have little effect on the total Cl content in the amphibole. This is seen in Fig. 6b where the Cl
435 content has no correlation with pressure. Given the large radius of Cl, it may be argued that

Always consult and cite the final, published document. See http:/www.minsocam.org or GeoscienceWorld

436 increased pressure will eventually act to exclude Cl from the amphibole structure. Preliminary
437 data on the upper-thermal stability of Cl-bearing amphibole with 0.5 Cl apfu (Jenkins, 2018)
438 indicates that it breaks down along a boundary that has a positive but steeper d*P*/d*T* slope than
439 the Cl-free equivalent. However, at this relatively low level of Cl, the predicted exclusion of Cl
440 with increased pressure has not yet been observed.

441 **Tetrahedral Al**

442 Although this study was not specifically designed to consider the effects of ^{T}Al, the range of
443 tetrahedral aluminum observed here is wider than anticipated and is at least worth considering.
444 Figure 8 shows the Cl content of all of the analyzed amphiboles reported in Table 3 plotted with
445 the same symbols as used in Figure 7. No clear correlation exists based on these samples. The
446 weight of evidence from field observations suggests that ^{T}Al can be important. This can be seen,
447 for example, for the zoned amphiboles in the peralkaline igneous complex of the Ramnes
448 cauldron, Norway (Sato et al., 1997), where ^{T}Al correlates with the Cl content. Unfortunately
449 ^{T}Al is often strongly coupled with A-site Na + K making it hard to decipher the effect of ^{T}Al by
450 itself. Based on the present study, ^{T}Al may not be the dominant control but it is present at a
451 fairly high level (1.4 - 1.6 ^{T}Al apfu, Fig. 8) in samples with reasonably high Cl content (0.6-0.9
452 Cl apfu) even when K is not present (Fig. 4).

453 **Implications**

454 A complete understanding of the crystal-chemical and physical conditions controlling the
455 incorporation of Cl into calcium amphiboles is well beyond the scope of this study because of
456 very limited experimental data on such things as the effects of ^{T}Al for calcium amphiboles,
457 variation of Cl content with Fe# [= $Fe^{2+}/(Fe^{2+} + Mg)$] for potassic-hastingsite, and the role of
458 variable brine concentration on hastingsitic amphiboles. Of the three chemical variations

Always consult and cite the final, published document. See http:/www.minsocam.org or GeoscienceWorld

commonly noted in the literature that correlate with Cl, namely the Fe#, ^{T}Al, and ^{A}K, this study can provide some insights on the latter two variables independent of the Fe#, which is fixed at 1.0 by virtue of the Mg-free bulk compositions studied here. The use of high brine concentrations in most of these syntheses also minimizes brine concentration as a variable (cf. Chan et al., 2016).

One thing that this study confirms is a direct correlation between K and Cl content, something that has not always been clearly determined from field studies alone. At a given set of *P*-*T*-f_{H2} conditions, amphiboles synthesized from bulk compositions that are identical in all aspects except for the ratio of Na to K in the A site clearly show that Cl is much higher in K- vs Na-rich amphiboles, with Cl contents getting up to about 1.2 apfu. This value, though well short of the theoretical 2.0 apfu, is certainly near the higher end of most terrestrial calcium amphiboles (e.g., Giesting and Filiberto, 2016). Henry and Daigle (2018) also observed the positive correlation between K and Cl content, but proposed that there was a minimum or threshold level of about 0.2 K apfu that needed to be reached before there was significant incorporation of Cl into the amphibole. In this study amphiboles without any K formed with Cl contents ranging from 0.6 – 0.9 apfu (Figs. 4, 5), so long as they formed in concentrated brines, which may be attributed to the high Fe# of 1.0 for all of these samples. As discussed below, there may well be a threshold value that exists owing to a coordinated effect from the ^{T}Al, Fe#, and K all reaching certain levels above which Cl can more readily enter the amphibole structure.

The possibility that different types of chloride salts may lead to variations in Cl contents has been considered in the literature. For example, the presence of $FeCl_2$ vs KCl in an ambient fluid has been suggested to give rise to different Cl concentrations in amphiboles (Liu et al., 2009). The implication from this study is that the chloride salt type is not important so long as the total

Always consult and cite the final, published document. See http:/www.minsocam.org or GeoscienceWorld

Cl content (i.e., brine concentration) and the bulk composition of the mixture are constant, as seen in Figure 4 when different combinations of NaCl, $CaCl_2$, and $FeCl_2$ are used. Replacing NaCl with KCl, however, would shift the bulk composition towards potassic hastingsite and correspondingly increase the Cl content (Fig. 5a).

The observation that many of the amphiboles synthesized from hastingsite bulk composition are deficient in total A-site cations and therefore plot within the hornblende field (Figs. 7a,b) was rather surprising. Hornblendes with considerable Cl (0.8 wt%) have been documented in meta-gabbros dredged from Mathematician Ridge west of the East Pacific Rise by Vanko (1986) and Kendrick et al. (2015). Based on the results of this study, it appears that A-site deficient hornblendes may form even in the presence of concentrated brines where there is adequate Na ± K to fill the A site. This was most noticeable for the (Na-rich) hastingsite bulk compositions (e.g., HAST 7-5, 7-6, 7-7; Table 3). The broader implication is that the A-site occupancy is not necessarily controlled by the availability of Na but rather by the ability of the amphibole to minimize its overall lattice energy through fairly specific substitutions of Fe, ^{T}Al, and Cl into its crystal structure.

Determining a general correlation between the crystal-chemistry of an amphibole and its Cl content is an important part of the broader goal of being able to use its Cl content to understand the conditions and brine chemistry that formed the amphibole. Even without a full understanding of the relative roles of ^{T}Al and K, one can combine their effects, along with the very strong control imposed by the Fe# (e.g., Kullerud, 1996; Liu et al., 2009; Henry and Daigle, 2018), to see if a correlation exists between the Cl content and the sum of ^{T}Al + K multiplied by the Fe# (called here the FeAlK index). Figure 9 shows amphiboles from this study (solid circles) that were formed from hastingsite bulk compositions, with and without K, compared to a

Always consult and cite the final, published document. See http:/www.minsocam.org or GeoscienceWorld

505 selection of amphiboles reported in the literature from metamorphic terranes. There is an overall
506 positive trend, and a linear regression to all of the data gives a correlation coefficient of 0.881.
507 There is also an initial range from 0 – 0.34 in the FeAlK index that is essentially devoid of Cl,
508 which agrees with the existence of a minimum or threshold in the Fe#, K, and ^{T}Al levels before
509 any significant Cl enters the amphibole structure reported by Henry and Daigle (2018). What is
510 particularly interesting is that the threshold level observed in Figure 9 includes data with a wide
511 range of Cl contents and localities, namely meta-gabbroic rocks of Lofoten, northern Norway
512 (Kullerud, 1996), and the meta-gabbroic rocks of the Bamble Sector, southern Norway
513 (Kusebauch et al., 2015), as well as the metamorphosed iron-formation samples reported by
514 Henry and Daigle (2018). This supports the hypothesis that there is a crystal-chemical minimum
515 in the FeAlK index that needs to be attained before significant Cl can enter the structure.
516 Additional work needs to be done to test this correlation and eventually to determine the
517 sensitivity of this FeAlK index to variations in the ambient fluid composition, which may
518 account for much of the spread in this diagram; however, this index is offered here as a first
519 approach to identifying a crystal-chemical parameter that may be applied to a wide range of
520 amphiboles.

521 **Acknowledgments**

522 The manuscript benefitted from the careful reviews of P. Ulmer and an anonymous reviewer.
523 David Collins assisted with the electron microprobe analyses. Financial support for this study
524 comes from NSF grants EAR-1347463 and EAR-1725053 to DMJ.

525 **References Cited**

526 Banno, Y., Miyawaki, R., Matsubara, S., Sato, E., Nakai, I., Matsuo, G., and Yamada, S. (2009)
527 Potassic-ferropargasite, a new member of the amphibole group, from Kabutoichiba, Mie

Always consult and cite the final, published document. See http:/www.minsocam.org or GeoscienceWorld

528 Prefecture, central Japan. Journal of the Mineralogical and Petrological Sciences, 104, 374-
529 382.
530 Barnes, J. D., and Cisneros, M. (2012) Mineralogical control on the chlorine isotope composition
531 of altered oceanic crust. Chemical Geology, 326-327, 51-60.
532 Barros, C. E. M., Sardinha, A. S., Barbosa, J. P. O., Macambira, M. J. B., Barbey, P., and
533 Boullier, A.-M. (2009) Structure, petrology, geochemistry and zircon U/Pb and Pb/Pb
534 geochronology of the synkinematic Archean (2.7 Ga) A-type granites from the Carajás
535 metallogenic province, northern Brazil. Canadian Mineralogist, 47, 1423-1440.
536 Bowen, N. L., and Schairer, J. F. (1935) Grünerite from Rockport, Massachusetts, and a series of
537 synthetic fluor-amphiboles. American Mineralogist, 20, 543-551.
538 Campanaro, B. P, and Jenkins, D. M. (2017) An experimental study of chlorine incorporation in
539 amphibole synthesized along the pargasite–ferro-pargasite join. Canadian Mineralogist, 55,
540 419-436.
541 Chan, A., Jenkins, D. M., and Dyar, M. D. (2016) Partitioning of chlorine between NaCl brines
542 and ferro-pargasite: Implications for the formation of chlorine-rich amphiboles in mafic
543 rocks. Canadian Mineralogist, 54, 337-351.
544 Chou, I-M. (1986) Permeability of precious metals to hydrogen at 2 kb of total pressure and
545 elevated temperatures. American Journal of Science, 286, 638-658.
546 Chou, I-M. (1987) Oxygen buffer and hydrogen sensor techniques at elevated pressures and
547 temperatures. In G.C. Ulmer and H. L. Barnes (eds.) Hydrothermal experimental techniques,
548 p. 61-99. Wiley, New York.
549 Comeforo, J. E., and Kohn, J. A. (1954) Synthetic asbestos investigations, I: Study of synthetic
550 fluor-tremolite. American Mineralogist, 39, 537-548.

Always consult and cite the final, published document. See http:/www.minsocam.org or GeoscienceWorld

551 Deer, W. A., Howie, R. A., and Zussman, J. (1997) Double-chain silicates. Rock Forming
552 Minerals, Vol. 2B, 2nd ed. The Geological Society, London, 764 pp.
553 Driscall, J., Jenkins, D.M., Dyar, M.D., and Bozhilov, K.N. (2005) Cation ordering in synthetic
554 low-calcium actinolite. American Mineralogist, 90, 900-911.
555 Enami, M., Liou, J. G., and Bird, D. K. (1992) Cl-bearing amphibole in the Salton Sea
556 geothermal system, California. Canadian Mineralogist, 30, 1077-1092.
557 Evans, B. W. (2007) The synthesis and stability of some end-member amphiboles. Reviews in
558 Mineralogy and Geochemistry, 67, 261-286.
559 Frezzotti, M. L., Ferrando, S., Peccerillo, A., Petrelli, M., Tecce. F., and Perucchi, A. (2011)
560 Chlorine-rich metasomatic H_2O-CO_2 fluids in amphibole-bearing peridotite from Injibara
561 (Lake Tana region, Ethiopian plateau): Nature and evolution of volatiles in the mantle of a
562 region of continental flood basalts. Geochimica et Cosmochimica Acta, 74, 3023-3039.
563 Frost, B. R. (1991) Introduction to oxygen fugacity and its petrologic importance. Reviews in
564 Mineralogy, 25, 1-9.
565 Giblin, L. E., Blackburn, W. H., and Jenkins, D. M. (1993) X-ray continuum discrimination
566 technique for the energy dispersive analysis of fine particles. Analytical Chemistry, 65,
567 3576-3580.
568 Giesting, P. A., and Filiberto, J. (2016) The formation environment of potassic-chloro-hastingsite
569 in the nakhlites MIL 03346 and pairs and NWA 5790: Insights from terrestrial chloro-
570 amphibole. Meteoritics and Planetary Science, 51, 2127-2153.
571 Gilbert, M. C. (1966) Synthesis and stability relations of the hornblende ferropargasite.
572 American Journal of Science, 264, 698-742.

Always consult and cite the final, published document. See http:/www.minsocam.org or GeoscienceWorld

573 Gilbert, M. C., Helz, R. T., Popp, R. K., and Spear, F. S. (1982) Experimental studies of
574 amphibole stability. Reviews in Mineralogy, 9B, 229-353.
575 Hari, K. R., Rao, N.V.C., Swarnkar, V., and Hou, G. (2014) Alkali feldspar syenites with
576 shoshonitic affinities from Chhotaudepur area: Implication for mantle metasomatism in the
577 Deccan large igneous province. Geoscience Frontiers, 5, 261-276.
578 Hawthorne, F. C., Oberti, R., Harlow, G. E., Maresch, W. V., Martin, R. F., Schumacher, J. C.,
579 and Welch, M. D. (2012) Nomenclature of the amphibole supergroup. American
580 Mineralogist, 97, 2031-2048.
581 Henry, D. J., and Daigle, N. M. (2018) Chlorine incorporation into amphibole and biotite in
582 high-grade iron-formations: Interplay between crystallography and metamorphic fluids.
583 American Mineralogist, 103, 55-68.
584 Hill, R. J. and Flack, H. D. (1987) The use of the Durbin-Watson *d* statistic in Rietveld analysis.
585 Journal of Applied Crystallography, 20, 356-361.
586 Holland, T. J. B. and Powell, R. (1990) An enlarged and updated internally consistent
587 thermodynamic dataset with uncertainties and correlations: the system K_2O-Na_2O-CaO-
588 MgO-MnO-FeO-Fe_2O_3-Al_2O_3-TiO_2-SiO_2-C-H-O_2. Journal of Metamorphic Geology, 8, 89-
589 124.
590 Holloway, J. R. & Wood, B. J. (1988) *Simulating the Earth: Experimental Geochemistry*.
591 Unwin Hyman, Inc., Boston, Massachusetts, 196 p.
592 Jenkins, D. M. (2018) The effect of Cl substitution on the thermal stability of ferro-pargasite.
593 Goldschmidt Abstracts, 2018.
594 Jenkins, D. M., and Corona, J. C. (2006) The role of water in the synthesis of glaucophane.
595 American Mineralogist, 91, 1055-1068.

Always consult and cite the final, published document. See http:/www.minsocam.org or GeoscienceWorld

596 Jenkins, D.M. and Hawthorne, F.C. (1995) Synthesis and Rietveld refinement of amphibole
597 along the join $Ca_2Mg_5Si_8O_{22}F_2$-$NaCa_2Mg_4Ga_3Si_6O_{22}F_2$. Canadian Mineralogist, 33:13-24.
598 Johnson, E. L., Goergen, E. T., Fruchey, B. L. (2004): Right lateral oblique slip movements
599 followed by post-Ottawan (1050-1020 Ma) orogenic collapse along the Carthage-Colton
600 shear zone: Data from the Dana Hill metagabbro body, Adirondack Mountains, New York.
601 In, R. P. Tollo, L. Corriveau, J. McLelland, and M. J. Bartholomew (eds.) Proterozoic
602 tectonic evolution of the Grenville orogeny in North America. Geological Society of
603 America. Memoir, 197, 357-378.
604 Kendrick, M. A., Honda, M., and Vanko, D. A. (2015) Halogens and noble gases in
605 Mathematician Ridge meta-gabbros, NE Pacific: implications for oceanic hydrothermal root
606 zones and global volatile cycles. Contributions to Mineralogy and Petrology, 170:43.
607 Kendrick M. A., Scambelluri, M., Hermann, J., Padrón-Navarta, J. A. (2018) Halogens and noble
608 gases in serpentinites and secondary peridotites: Implications for seawater subduction and
609 the origin of mantle neon. Geochimica et Cosmochimica Acta, 235, 285-304.
610 Kullerud, K. (1996) Chlorine-rich amphiboles: interplay between amphibole composition and an
611 evolving fluid. European Journal of Mineralogy, 8, 355-370.
612 Kusebauch, C., John, T., Barnes, J. D., Klügel, A., and Austrheim, H. O. (2015) Halogen
613 element and stable chlorine isotope fractionation caused by fluid-rock interaction (Bamble
614 Sector, SE Norway). Journal of Petrology, 56, 299-324.
615 Larson, A.C., and Von Dreele, R.B. (2000) General Structure Analysis System (GSAS), Los
616 Alamos National Lab Report (LAUR) 86-748.

Always consult and cite the final, published document. See http:/www.minsocam.org or GeoscienceWorld

617 Liogys, V. A., and Jenkins, D. M. (2000) Hornblende geothermometry of amphibolite layers of
618 the Popple Hill gneiss, north-west Adirondack Lowlands, New York, USA. Journal of
619 Metamorphic Geology, 18, 513-530.
620 Liu, Jingbo, Liu, Wenyuan, Ye, Kai, and Mao, Qian (2009) Chlorine-rich amphibole in Yangkou
621 eclogite, Sulu ultrahigh-pressure metamorphic terrane, China. European Journal of
622 Mineralogy, 21, 1265-1285.
623 Makino, K., Tomita, K., and Suwa, K. (1993) Effect of chlorine on the crystal structure of a
624 chlorine-rich hastingsite. Mineralogical Magazine, 57, 677-685.
625 Mandler, B. E., and Grove, T. L. (2016) Controls on the stability and composition of amphibole
626 in the Earth's mantle. Contributions to Mineralogy and Petrology, 171, 68.
627 Mazdab, F. M. (2003) The diversity and occurrence of potassium-dominant amphiboles.
628 Canadian Mineralogist, 41, 1329-1344.
629 McCormick, K. A. and McDonald, A. M. (1999) Chlorine-bearing amphiboles from the Fraser
630 Mine, Sudbury Ontario, Canada: Description and crystal chemistry. Canadian Mineralogist,
631 37, 1385-1403.
632 McCubbin, F. M., Elardo, S. M., Shearer, C. K., Jr., Smirnov, A. Hauri, E. H., and Draper, D. S.
633 (2013) A petrogenetic model for the comagmatic origin of chassignites and nakhlites:
634 Inferences from chlorine-rich minerals, petrology, and geochemistry. Meteoritics and
635 Planetary Science, 48, 819-853.
636 Morrison, J. (1991) Compositional constraints on the incorporation of Cl into amphiboles.
637 American Mineralogist, 76, 1920-1930.

Always consult and cite the final, published document. See http:/www.minsocam.org or GeoscienceWorld

638 Mueller, B. L., Jenkins, D. M., and Dyar, M. D. (2017) Chlorine incorporation in amphiboles
639 synthesized along the magnesio-hastingsite–hastingsite compositional join. European
640 Journal of Mineralogy, 29, 167-180.
641 Pagano, D. S., Galliski, M. A., Márquez-Zavalía, M. F., and Colombo, F. (2016) Petrology and
642 mineralogy of the La Peña igneous complex, Mendoza, Argentina: An alkaline occurrence in
643 the Miocene magmatism of the Southern Central Andes. Journal of the South American
644 Earth Sciences, 67,158-179.
645 Pavlovich, M. S., Jr., and Jenkins, D. M. (2003) Assessment of cation substitutions along the
646 gallium and fluorine analogue of the tremolite-glaucophane join. American Mineralogist, 88,
647 1486-1495.
648 Pownceby, M. & O'Neill, H. (2000): Thermodynamic data from redox reactions at high
649 temperatures. VI. Thermodynamic properties of CoO-MnO solid solutions from emf
650 measurements. Contributions to Mineralogy and Petrology, 140, 28-39.
651 Raudsepp, M., Turnock, A. C., and Hawthorne, F. C. (1991) Amphibole synthesis at low
652 pressure: what grows and what doesn't. European Journal of Mineralogy, 3, 983-1004.
653 Robert, J.-L., Della Ventura, G., and Thauvin, J.-L. (1989) The infrared OH-stretching region of
654 synthetic richterites in the system Na_2O-K_2O-CaO-MgO-SiO_2-H_2O-HF. European Journal of
655 Mineralogy, 1, 203-211.
656 Selverstone, J. and Sharp, Z. D. (2011) Chlorine isotope evidence for multicomponent mantle
657 metasomatism in the Ivrea Zone. Earth and Planetary Science Letters, 310, 429-440.
658 Sharma, A., and Jenkins, D. M. (1999) Hydrothermal synthesis of amphiboles along the
659 tremolite-pargasite join and in the ternary system tremolite-pargasite-cummingtonite.
660 American Mineralogist, 84, 1304-1318.

Always consult and cite the final, published document. See http:/www.minsocam.org or GeoscienceWorld

661 Shaw, H.R., and Wones, D.R. (1964) Fugacity coefficients for hydrogen gas between 0° and
662 1000°C for pressures to 3000 atm. American Journal of Science, 262, 918-929.

663 Thomas, W. A. (1982) Stability relations of the amphibole hastingsite. American Journal of
664 Science, 282, 136-164.

665 Tropper, P., Manning, C. E., Essene, E. J., and Kao, L.-S. (2000) The compositional variation of
666 synthetic sodic amphiboles at high and ultra-high pressures. Contributions to Mineralogy
667 and Petrology, 139, 146-162.

668 Vanko, D. A. (1986) High-chlorine amphiboles from oceanic rocks: product of highly-saline
669 hydrothermal fluids? American Mineralogist, 71, 51-59.

670 Weidner, J. R. (1989) Welding silver and silver alloy containers for high-temperature and high-
671 pressure experiments. American Mineralogist, 74, 1385.

672

Always consult and cite the final, published document. See http:/www.minsocam.org or GeoscienceWorld

This is a preprint, the final version is subject to change, of the American Mineralogist (MSA)
Cite as Authors (Year) Title. American Mineralogist, in press.
DOI: https://doi.org/10.2138/am-2019-6768

673

674 Table 1. Nominal anhydrous compositions investigated in this study

Sample Code Prefix	Cl-source	Nominal anhydrous composition, comments
Ferro-pargasite		
FEPG 1	"$FeCl_2$"	$NaCa_2(Fe_{4.0}Al)(Al_2Si_6)O_{22}(Cl_2)$
FEPG 3	no Cl	$NaCa_2(Fe_{4.0}Al)(Al_2Si_6)O_{23}$
Hastingsite		
HAST 5	"$FeCl_2$"	$Na(Ca_{1.8}Fe_{0.2})[Fe_{4.0}(Fe^{3+}{}_{0.8}Al_{0.2})](Al_2Si_6)O_{22}Cl_2$
HAST 6	"$FeCl_2$"	$(K_{0.2}Na_{0.8})(Ca_{1.8}Fe_{0.2})[Fe_{4.0}(Fe^{3+}{}_{0.8}Al_{0.2})](Al_2Si_6)O_{22}Cl_2$
HAST 7	"$FeCl_2$"	$(K_{0.4}Na_{0.6})(Ca_{1.8}Fe_{0.2})[Fe_{4.0}(Fe^{3+}{}_{0.8}Al_{0.2})](Al_2Si_6)O_{22}Cl_2$
HAST 8	"$FeCl_2$"	$(K_{0.6}Na_{0.4})(Ca_{1.8}Fe_{0.2})[Fe_{4.0}(Fe^{3+}{}_{0.8}Al_{0.2})](Al_2Si_6)O_{22}Cl_2$
HAST 10	$CaCl_2$	$(K_{0.6}Na_{0.4})Ca_2(Fe_{4.0}Fe^{3+})(Al_2Si_6)O_{22}Cl_2$
HAST 9	"$FeCl_2$"	$(K_{0.8}Na_{0.2})(Ca_{1.8}Fe_{0.2})[Fe_{4.0}(Fe^{3+}{}_{0.8}Al_{0.2})](Al_2Si_6)O_{22}Cl_2$
HAST 11	"$FeCl_2$"	$K(Ca_{1.8}Fe_{0.2})[Fe_{4.0}(Fe^{3+}{}_{0.8}Al_{0.2})](Al_2Si_6)O_{22}Cl_2$
HAST 12	"$FeCl_2$"	$NaCa_2(Fe_{4.0}Fe^{3+})(Al_2Si_6)O_{22}Cl_2$
HAST 13	$CaCl_2$	$NaCa_2(Fe_{4.0}Fe^{3+})(Al_2Si_6)O_{22}Cl_2$
HAST 14	NaCl+½"$FeCl_2$"	$NaCa_2(Fe_{4.0}Fe^{3+})(Al_2Si_6)O_{22}Cl_2$, two sources of Cl
HAST 15	NaCl+½$CaCl_2$	$NaCa_2(Fe_{4.0}Fe^{3+})(Al_2Si_6)O_{22}Cl_2$, two sources of Cl

675

676

677

Always consult and cite the final, published document. See http:/www.minsocam.org or GeoscienceWorld

This is a preprint, the final version is subject to change, of the American Mineralogist (MSA)
Cite as Authors (Year) Title. American Mineralogist, in press.
DOI: https://doi.org/10.2138/am-2019-6768

678 Table 2. Synthesis conditions and products of synthesis for bulk compositions listed in Table 1.

Sample Code	T (°C)	P (GPa)	t (hrs)	$\Delta\log(f_{O2})$[a]	$\log(f_{H2})$[b]	brine[b] (X_{Cl})	Products and comments
Amphibole formation in P-T-f_{H2} space							
FEPG 1-2	700(5)	0.197(5)	265	-1.4(5)	[1.8(3)]	0.47(3)	plag, fay, cpx, halite, qtz, $FeCl_2 \cdot nH_2O$
FEPG 1-6	607(5)	0.196(5)	506	-0.9(1)	[1.4(1)]	0.40(1)	amph, plag, halite, $FeCl_2 \cdot nH_2O$
FEPG 1-9	600(4)	0.202(6)	168	*-1.26(3)*	1.37(2)	0.34(1)	plag, amph, cpx, fay, halite, $FeCl_2 \cdot nH_2O$
FEPG 1-10	949(3)	0.210(5)	144	-0.93(3)	1.84(1)	0.54(2)	plag, cpx, fay, halite, $FeCl_2 \cdot nH_2O$; capsule is $Ag_{70}Pd_{30}$
FEPG 1-11	600(5)	0.204(5)	365	-0.9(1)	[1.4(1)]	0.44(3)	amph, plag, halite, $FeCl_2 \cdot nH_2O$
FEPG 1-13	599(5)	0.205(5)	456	*-0.88(10)*	[1.4(1)]	0.52(1)	plag, mt, cpx, halite, amph, qtz, $FeCl_2 \cdot nH_2O$; capsule is $Ag_{70}Pd_{30}$
FEPG 1-14	600(5)	0.202(5)	357	-0.9(1)	[1.4(1)]	0.61(4)	amph, plag, fay, halite, $FeCl_2 \cdot nH_2O$; capsule is $Ag_{50}Pd_{50}$
FEPG 1-16	600(5)	0.207(5)	312	-0.9(1)	[1.4(1)]	0.57(3)	plag, mt, cpx, qtz, halite, $FeCl_2 \cdot nH_2O$; capsule is Au
FEPG 1-17	600(5)	0.201(5)	311	-0.9(1)	[1.4(1)]	0.84(16)	plag, mt, cpx, qtz, halite, $FeCl_2 \cdot nH_2O$; capsule is Pt
FEPG 1-8	698(6)	0.416(5)	197	-1.38(3)	2.04(2)	0.30(2)	plag, cpx, amph, halite, qtz, fay, $FeCl_2 \cdot nH_2O$
FEPG 1-7	798(7)	0.450(5)	342	-1.72(2)	2.37(1)	0.26(3)	plag, cpx, halite, qtz, $FeCl_2 \cdot nH_2O$
Variable brine conc.							
FEPG 3-16	699(5)	0.200(5)	481	-1.4(5)	[1.8(3)]	0.0	plag, cpx, mt, gt
FEPG 3-17	700(5)	0.202(5)	146	-1.4(5)	[1.8(3)]	0.0	amph, plag, cpx
FEPG 3-12	700(5)	0.204(5)	317	-1.4(5)	[1.8(3)]	0.018(2)	cpx, plag, mt
FEPG 3-13	700(5)	0.200(5)	353	-1.4(5)	[1.8(3)]	0.036(2)	cpx, plag, mt
FEPG 3-14	700(5)	0.196(5)	408	-1.4(5)	[1.8(3)]	0.070(2)	amph, cpx, plag, fay, $FeCl_2 \cdot nH_2O$
FEPG 3-15	700(5)	0.200(5)	363	-1.4(5)	[1.8(3)]	0.110(2)	amph, plag, cpx, fay

Always consult and cite the final, published document. See http:/www.minsocam.org or GeoscienceWorld

Amphibole formation with T							
FEPG 3-5	700(5)	0.194(7)	672	-1.4(5)	[1.8(3)]	0.46(3) NaCl	amph, plag, cpx, halite, gt
FEPG 3-19	753(6)	0.200(8)	451	-1.4(5)	[1.9(2)]	0.31(1) NaCl	amph, plag, cpx, halite
FEPG 3-18	800(5)	0.203(6)	143	-1.4(5)	[1.9(2)]	0.318(3) NaCl	amph, plag, cpx, halite
FEPG 3-21	850(4)	0.200(5)	219	-0.87(3)	1.73(2)	0.20(2) NaCl	plag, amph, cpx, halite
FEPG 3-20	899(7)	0.202(5)	119	*-2.1(1)*	1.77(2)	0.58(7) NaCl	amph, cpx, plag, halite
FEPG 3-22	950(5)	0.200(5)	142	-0.91(3)	1.82(2)	0.24(1) NaCl	plag, cpx, halite
Variable chloride salts in hastingsite							
HAST 12-1	700(3)	0.43(2)	168	-1.46(4)	2.09(2)	1.00(6) $FeCl_2$	amph, fay, cpx, qtz, halite, plag, $FeCl_2 \cdot nH_2O$
HAST 13-1	700(3)	0.43(2)	168	-1.46(4)	2.09(2)	1.00(8) $CaCl_2$	cpx, amph, fay, gt, qtz, $CaCl_2 \cdot nH_2O$
HAST 14-1	700(3)	0.43(2)	168	-1.46(4)	2.09(2)	0.95(4) NaCl + $FeCl_2$	amph, fay, cpx, gt, qtz, plag, $FeCl_2 \cdot nH_2O$, halite
HAST 15-1	700(3)	0.43(2)	168	-1.46(4)	2.09(2)	0.97(4) NaCl + $CaCl_2$	cpx, gt, fay,hast, plag, halite, $CaCl_2 \cdot nH_2O$
K-Na substitution in hastingsite							
HAST 5-2	700(6)	0.450(5)	120	*-1.33(4)*	2.10(2)	0.50(3)	amph, plag, qtz, fay
HAST 6-2	700(3)	0.465(5)	262	*-1.30(4)*	2.13(2)	0.83(7)	amph
HAST 7-2	700(3)	0.465	262	*-1.30(4)*	2.13(2)	0.72(5)	amph, gt, qtz
HAST 8-2	700(7)	0.368(5)	111	-1.29(4)	1.98(2)	0.89(9)	amph, fay, qtz, plag, cpx
HAST 10-1	700(5)	0.345(5)	263	-1.26(4)	1.92(2)	0.91(8)	amph, cpx, fay, qtz, plag
HAST 9-2	700(7)	0.368(5)	111	-1.29(4)	1.98(2)	0.88(8)	amph, fay, qtz
HAST 11-1	700(3)	0.422(5)	116	-1.38(4)	2.05(2)	0.91(3)	amph, fay, qtz
Amphibole formation with P							

Always consult and cite the final, published document. See http:/www.minsocam.org or GeoscienceWorld

HAST 7-3	700(3)	0.102(5)	232	-1.23(3)	1.55(2)	0.96(4)	plag, cpx, fay, qtz, halite, $FeCl_2 \cdot nH_2O$
HAST 7-4	700(4)	0.206(5)	163	*-2.2(1)*	1.77(4)	0.95(3)	plag, cpx, fay, amph, qtz, halite, sylvite, $FeCl_2 \cdot nH_2O$
HAST 7-5	700(5)	0.300(5)	116	-1.33(4)	1.91(2)	0.97(3)	amph, plag, cpx, fay, halite, qtz, $FeCl_2 \cdot nH_2O$
HAST 7-6	700(5)	0.38(2)	171	-1.34(5)	1.99(4)	0.98(4)	amph, plag, fay, qtz, halite, $FeCl_2 \cdot nH_2O$
HAST 7-7	701(8)	0.455(6)	163	-1.37(6)	2.07(3)	> 0.79	amph, gt, fay, plag, qtz, halite, $FeCl_2 \cdot nH_2O$

Note: Uncertainties in the last digit are given in parentheses. Products are listed in decreasing abundance as estimated from the powder XRD patterns. Abbreviations: amph = amphibole, cpx = hedenbergitic clinopyroxene, fay = fayalite, gt = garnet, mt = magnetite, plag = plagioclase, qtz = quartz.

[a]Oxygen fugacity (f_{O2}) indicated as log(f_{O2}) relative to that of the fayalite-magnetite-β-quartz (FMβQ) oxygen buffer of Frost (1991). Values in italics were determined using the variable oxygen fugacity sensor assemblage Co-MnO-CoO of Pownceby and O'Neill (2000).

[b]Hydrogen fugacities, indicated as log(f_{H2}), are those imposed by a H_2-Ar mixture as described in the text; values in brackets were calculated from given f_{O2}.

[c]X_{Cl} = mole fraction of Cl in any brine that may be present, either from moisture absorbed by the salt in the starting mixture, or in a brine purposely added. For syntheses which were nominally anhydrous, this value represents the total mass of the salt initially present in the starting mixture and the mass of water present at the end of the synthesis, assessed by weight lost upon drying the opened capsule. Unless stated differently, the salt in these syntheses is $FeCl_2$.

.

Always consult and cite the final, published document. See http:/www.minsocam.org or GeoscienceWorld

This is a preprint, the final version is subject to change, of the American Mineralogist (MSA)
Cite as Authors (Year) Title. American Mineralogist, in press.
DOI: https://doi.org/10.2138/am-2019-6768

694 Table 3. Electron microprobe analyses of amphiboles synthesized in this study at the conditions indicated in Table 2. Ferric iron
695 contents were fixed at 18% as discussed in the text.

Oxide/atom	Sample code							
wt%	FEPG 3-5	FEPG 3-19	FEPG 3-18	FEPG 3-21	FEPG 3-20	HAST 12-1	HAST 13-1	HAST 14-1
n	8	17	14	16	17	20	16	16
SiO_2	36.1(12)	37.2(9)	36.8(9)	36.8(13)	36.8(30)	38.6(26)	36.5(27)	35.8(39)
Al_2O_3	13.4(4)	14.1(7)	14.5(6)	15.5(3)	15.4(5)	11.2(18)	10.8(23)	9.97(23)
FeO[a]	31.8(8)	32.8(9)	33.2(4)	31.1(12)	32.2(5)	31.3(11)	31.3(27)	29.2(28)
CaO	11.2(4)	10.9(3)	11.1(2)	10.8(3)	11.1(3)	9.85(68)	9.16(97)	9.16(12)
Na_2O	3.34(9)	3.53(16)	3.59(15)	3.56(19)	3.39(11)	2.43(21)	2.53(42)	2.35(28)
Cl	0.34(4)	0.30(5)	0.23(3)	0.22(3)	0.40(3)	2.75(31)	3.04(52)	2.53(27)
Total	96.7(23)	98.9(20)	99.5(15)	97.9(30)	99.4(10)	96.9(42)	93.9(51)	89.6(82)
Total –Cl=O	96.7(23)	98.8(2)	99.4(15)	97.9(30)	99.3(10)	96.3(42)	93.3(50)	89.0(82)
atoms								
Si	5.98(8)	5.95(11)	5.86(8)	5.90(5)	5.84(5)	6.43(27)	6.34(26)	6.47(32)
Al-T	2.02(8)	2.05(11)	2.14(8)	2.10(5)	2.16(5)	1.57(27)	1.66(26)	1.53(32)
Sum T	8.00	8.00	8.00	8.00	8.00	8.00	8.00	8.00

Always consult and cite the final, published document. See http:/www.minsocam.org or GeoscienceWorld

This is a preprint, the final version is subject to change, of the American Mineralogist (MSA)
Cite as Authors (Year) Title. American Mineralogist, in press.
DOI: https://doi.org/10.2138/am-2019-6768

Al-C	0.60(5)	0.61(9)	0.57(7)	0.83(5)	0.73(5)	0.65(14)	0.53(26)	0.60(24)
Fe^{3+}-C	0.79(1)	0.79(2)	0.80(1)	0.75(1)	0.77(1)	0.78(3)	0.82(7)	0.80(5)
Fe^{2+}-C	3.61(4)	3.60(7)	3.63(6)	3.42(4)	3.50(4)	3.57(11)	3.65(20)	3.60(19)
Sum C	5.00	5.00	5.00	5.00	5.00	5.00	5.00	5.00
Fe-B	0.0	0.01(2)	0.00	0.00	0.00	0.01(2)	0.08(13)	0.03(8)
Ca-B	1.98(3)	1.87(5)	1.89(4)	1.85(3)	1.88(5)	1.76(9)	1.70(14)	1.77(12)
Na-B	0.02(3)	0.12(4)	0.10(4)	0.15(3)	0.12(5)	0.24(9)	0.22(11)	0.20(11)
Sum B	2.00	2.00	2.00	2.00	2.00	2.00	2.00	2.00
Na-A	1.05(3)	0.97(3)	1.00(3)	0.96(5)	0.92(4)	0.55	0.62(11)	0.63(13)
Ca-A	0.00	0.00	0.00	0.00	0.00	0.00	0.01(2)	0.00(1)
Total cations	16.06(3)	15.98(3)	16.00(3)	15.96(6)	15.93(4)	15.55(9)	15.64(10)	15.64(14)
Cl	0.094(13)	0.083(14)	0.062(7)	0.061(9)	0.109(7)	0.77(8)	0.89(14)	0.78(6)
OH^b	1.49(11)	1.71(20)	1.82(11)	1.64(10)	1.75(9)	1.06(21)(	1.00(24)	0.91(32)

696

Always consult and cite the final, published document. See http:/www.minsocam.org or GeoscienceWorld

This is a preprint, the final version is subject to change, of the American Mineralogist (MSA)
Cite as Authors (Year) Title. American Mineralogist, in press.
DOI: https://doi.org/10.2138/am-2019-6768

697 Table 3 (continued)

Oxide/atom	Sample code							
wt%	HAST 15-1	HAST 5-2	HAST 6-2	HAST 7-2	HAST 8-2	HAST 10-1	HAST 9-2	HAST 11-1
n	7	11	14	12	13	23	12	9
SiO_2	33.0(28)	41.0(9)	39.9(19)	38.7(18)	39.7(15)	38.7(21)	39.2(22)	37.5(17)
Al_2O_3	12.1(31)	10.4(8)	12.3(21)	11.1(24)	10.7(9)	10.4(10)	10.4(4)	11.2(19)
FeO[a]	31.4(32)	32.7(11)	33.2(25)	33.3(17(	31.8(12)	32.9(13)	32.5(17)	30.7(13)
CaO	8.04(18)	10.7(6)	8.9(10)	9.5(12)	10.7(6)	10.6(9)	10.8(6)	10.6(6)
Na_2O	2.21(61)	2.07(18)	1.42(22)	0.93(25)	0.81(13)	1.07(11)	0.34(5)	0.09(3)
K_2O	----	0.01(1)	0.52(12)	1.52(52)	2.50(15)	2.00(25)	3.40(16)	3.99(25)
Cl	1.98(56)	2.19(13)	1.63(19)	1.94(40)	2.48(21)	3.26(26)	3.06(21)	4.04(25)
Total	89.4(62)	99.1(17)	98.1(40)	97.0(47)	98.8(20)	99.0(32)	94.3(38)	98.3(20)
Total –Cl=O	88.3(62)	98.6(17)	97.6(39)	96.6(46)	98.2(20)	98.3(32)	98.9(32)	97.4(20)
atoms								
Si	5.99(26)	6.61(11)	6.42(19)	6.39(19)	6.54(12)	6.42(19)	6.49(19)	6.42(24)
Al-T	2.01(26)	1.39(11)	1.58(19(	1.61(19)	1.46(12)	1.58(19)	1.51(19)	1.58(24)
Sum T	8.00	8.00	8.00	8.00	8.00	8.00	8.00	8.00

Always consult and cite the final, published document. See http:/www.minsocam.org or GeoscienceWorld

Al-C	0.56(35)	0.59(9)	0.75(24)	0.55(28)	0.62(16)	0.46(16)	0.52(15)	0.68(19)
Fe^{3+}-C	0.86(10)	0.79(2)	0.80(6)	0.83(5)	0.79(3)	0.82(4)	0.81(4)	0.79(5)
Fe^{2+}-C	3.58(25)	3.62(8)	3.45(18)	3.63(24)	3.59(13)	3.72(12)	3.67(12)	3.53(14)
Sum C	5.00	5.00	5.00	5.00	5.00	5.00	5.00	5.00
Fe-B	0.35(26)	0.00	0.22(12)	0.14(12)	0.00(2)	0.03(7)	0.02(8)	0.08(11)
Ca-B	1.55(26)	1.85(10)	1.54(15)	1.67(17)	1.88(10)	1.87(10)	1.91(10)	1.91(10)
Na-B	0.10(8)	0.15(10)	0.25(9)	0.18(8)	0.12(9)	0.10(9)	0.06(4)	0.01(1)
Sum B	2.00	2.00	2.00	1.99(2)	2.00	2.00	1.99(1)	2.00(1)
Ca-A	0.00	0.00	0.00	0.00	0.01(2)	0.02(5)	0.00(1)	0.04(6)
Na-A	0.68(18)	0.49(9)	0.19(9)	0.12(9)	0.14(9)	0.24(8)	0.05(4)	0.02(2)
K-A	----	0.00	0.11(2)	0.32(10)	0.52(3)	0.42(5)	0.72(4)	0.87(4)
Total cations	15.69(18)	15.49(9)	15.30(10)	15.43(16)	15.67(12)	15.69(10)	15.77(8)	15.92(9)
Cl	0.61(16)	0.60(3)	0.44(4)	0.54(11)	0.69(6)	0.92(8)	0.86(6)	1.17(6)
OH^b	1.39(19)	1.07(29)	1.53(8)	1.46(11)	0.80(26)	0.77(30)	0.62(39)	0.00

698
699

Always consult and cite the final, published document. See http:/www.minsocam.org or GeoscienceWorld

This is a preprint, the final version is subject to change, of the American Mineralogist (MSA)
Cite as Authors (Year) Title. American Mineralogist, in press.
DOI: https://doi.org/10.2138/am-2019-6768

700 Table 3 (continued)

Oxide/atom wt%	Sample code			
	HAST 7-4	HAST 7-5	HAST 7-6	HAST 7-7
n	14	21	13	10
SiO_2	37.2(42)	41.1(19)	40.6(17)	38.4(19)
Al_2O_3	8.8(14)	9.0(13)	9.2(15)	9.9(16)
FeO[a]	32.8(18)	36.2(17)	35.2(17)	33.4(16)
CaO	9.3(12)	9.3(12)	9.1(8)	9.1(9)
Na_2O	0.81(15)	0.71(12)	0.80(14)	0.89(19)
K_2O	1.16(27)	1.11(32)	1.33(38)	1.66(37)
Cl	1.71(27)	1.48(28)	1.57(22)	1.67(29)
Total	91.8(64)	98.8(24)	97.8(22)	95.1(35)
Total –Cl=O	91.4(64)	98.5(24)	97.5(22)	94.7(35)
atoms				
Si	6.53(34)	6.66(21)	6.63(23)	6.48(23)
Al-T	1.47(34)	1.34(21)	1.37(23)	1.52(23)
Sum T	8.00	8.00	8.00	8.00

Always consult and cite the final, published document. See http:/www.minsocam.org or GeoscienceWorld

Al-C	0.36(24)	0.37(12)	0.41(15)	0.45(13)
Fe^{3+}-C	0.87(5)	0.88(3)	0.86(3)	0.85(3)
Fe^{2+}-C	3.77(19)	3.75(11)	3.72(12)	3.70(10)
Sum C	5.00	5.00	5.00	5.00
Fe-B	0.20(16)	0.26(17)	0.22(14)	0.16(11)
Ca-B	1.71(14)	1.60(19)	1.60(16)	1.63(14)
Na-B	0.09(9)	0.14(6)	0.18(5)	0.20(5)
Sum B	2.00	2.00	2.00	2.00
Ca-A	0.04(9)	0.01(4)	0.0	0.0
Na-A	0.18(10)	0.09(7)	0.07(6)	0.09(9)
K-A	0.26(6)	0.23(7)	0.28(8)	0.36(7)
Total cations	15.48(14)	15.33(14)	15.34(14)	15.44(15)
Cl	0.51(8)	0.41(8)	0.44(6)	0.48(8)
OH[b]	1.29(38)	1.49(17)	1.51(11)	1.51(10)

Values reported are the average of *n* analyses, and uncertainties (1σ) in the last digit given in parentheses.
[a] Total Fe reported as FeO
[b] Estimated by adding sufficient OH to either have the sum of OH+Cl in the W sites equal 2.0, or the sum of T- and C-site cations (excluding Ca, Na, and K) equal 13.

Always consult and cite the final, published document. See http:/www.minsocam.org or GeoscienceWorld

This is a preprint, the final version is subject to change, of the American Mineralogist (MSA)
Cite as Authors (Year) Title. American Mineralogist, in press.
DOI: https://doi.org/10.2138/am-2019-6768

706 Figure Captions

707

708 Figure 1. (a) Log(f_{O2}) calculated from the imposed hydrogen fugacity as a function of the
709 observed value of log(f_{O2}) for selected experiments for which the oxygen fugacity was
710 determined using the method of Pownceby and O'Neill (2000). Diagonal line represents
711 one-to-one correlation, numbers indicate the duration of each treatment in hours, and the grey
712 circle is an experiment near the upper-limit of the sensor method. (b) Proposed stability field
713 of Cl-bearing amphiboles (solid curve) synthesized from ferro-chloro-pargasite in this study
714 (FEPG 1-x, FEPG 3-x, Table 2) compared with the stability field of (hydroxyl) ferro-
715 pargasite reported by Gilbert (1966) at 0.2 GPa (dashed curve), the latter converted from the
716 originally reported log(f_{O2})-T to equivalent log(f_{H2})-T space as discussed in the text. Solid
717 symbols indicate growth of amphibole, open symbols indicate no amphibole growth, and
718 half-shaded symbol indicates mixed results. Experiments were done at 0.2 GPa unless
719 indicated otherwise.

720 Figure 2. Proportion of amphibole (wt%) synthesized from the ferro-pargasite bulk composition
721 as a function of the $FeCl_2$ brine concentration, expressed as the mole fraction of $FeCl_2$ [
722 $X_{FeCl_2}^{brine}$ = moles $FeCl_2$/(moles $FeCl_2$ + moles H_2O)]. Open circles indicate coexisting
723 magnetite (+ Mt), solid circles indicate coexisting fayalite (+ Fay), and the square indicates
724 amphibole growth but has neither coexisting magnetite nor fayalite (FEPG 3-17, Table 2).

725 Figure 3. (a) Chlorine content (apfu) of amphibole synthesized at 0.2 GPa from ferro-pargasite
726 bulk composition as a function of the temperature of synthesis. (b) Cl content of amphibole
727 versus the NaCl brine concentration of the bulk mixture, determined after the synthesis as
728 described in the text. Points are labeled with the corresponding sample code from Table 2.

Always consult and cite the final, published document. See http:/www.minsocam.org or GeoscienceWorld

729 Figure 4. Chlorine contents of amphibole synthesized from chloro-hastingsite bulk compositions
730 made using different combinations of salts, here indicated by the moles of $FeCl_2$ used in the
731 starting mixture. All syntheses were done together at 700°C and 0.43 GPa for 168 h at a
732 fugacity of H_2 equivalent to $\Delta\log(f_{O2})$ = -1.46 FMβQ . The chloride salts used instead of, or
733 along with, $FeCl_2$ are indicated next to each data point. Bold horizontal line indicates the
734 average Cl content of all experiments, while the thin horizontal lines indicate the standard
735 deviation (± 1σ) about the average.
736 Figure 5. (a) Chlorine content (apfu) of hastingsitic amphiboles plotted against their K content
737 and labeled with the individual sample codes in Tables 2 and 3. Line is a linear regression to
738 all data with a correlation coefficient r = 0.836. (b) Chlorine content plotted against the mole
739 fraction of Cl in the brine (X_{Cl}). A linear regression to these data yield a much poorer
740 correlation (r = 0.530) indicating that K, rather than brine concentration, is the dominant
741 influence on Cl content.
742 Figure 6. (a) Dependence of amphibole yield (wt%) on pressure at 700°C and $\log(f_{O2})$ 1.2 – 2.2
743 below FMβQ. Bulk composition of the starting mixture is
744 $(K_{0.4}Na_{0.6})(Ca_{1.8}Fe_{0.2})[Fe_{4.0}(Fe^{3+}_{0.8}Al_{0.2})](Al_2Si_6)O_{22}Cl_2$ with coexisting phases being
745 dominantly hedenbergite, fayalite, and plagioclase. Circles are labeled with the
746 corresponding sample codes in Table 2. (b) Chlorine content (apfu) of the same amphiboles
747 in (a) plotted as a function of the pressure of synthesis.
748 Figure 7. Classification of amphiboles synthesized in this study based on Hawthorne et al.
749 (2012) for ^{W}(OH,F,Cl)-dominant calcium amphiboles. (a) Open circles are synthetic
750 amphiboles made from a mixture of ferro-pargasite bulk composition (solid circle) over the
751 temperature range of 700 – 900°C at 0.43 GPa. Arrow indicates the general trend of

Always consult and cite the final, published document. See http:/www.minsocam.org or GeoscienceWorld

752 increasing temperature (*T*). Open squares are amphiboles made from mixtures of hastingsite
753 composition (solid square) but using different chloride salts or combinations of salts. Grey
754 squares are amphiboles synthesized at 700°C over the pressure range of 0.1 to 0.45 GPa all
755 from a hastingsite bulk composition having 40% substitution of K for Na. There is no
756 discernible trend with pressure. (b) Amphiboles made from an Al-enriched hastingsite bulk
757 composition (solid diamond) for which K was substituted for Na in the A site in 20 mol%
758 increments. Arrow indicates increasing K content.
759 Figure 8. Chlorine content(apfu) of synthetic amphiboles as a function of their tetrahedral Al
760 content (^{T}Al, apfu). Samples and symbols are the same as those in Fig. 7.
761 Figure 9. Chlorine content (apfu) as a function of the FeAlK index proposed in this study (see
762 text) for a selection of natural calcium amphiboles from various meta-gabbroic and
763 metamorphosed iron-formation rocks as well as synthetic amphiboles made from hastingsite
764 bulk compositions (solid circles) in this study. Diagonal line is the linear regression to all of
765 the data with the correlation coefficient (*r*) and resultant equation given in the figure.
766

Always consult and cite the final, published document. See http:/www.minsocam.org or GeoscienceWorld

This is a preprint, the final version is subject to change, of the American Mineralogist (MSA)
Cite as Authors (Year) Title. American Mineralogist, in press.
DOI: https://doi.org/10.2138/am-2019-6768

767 Figure 1

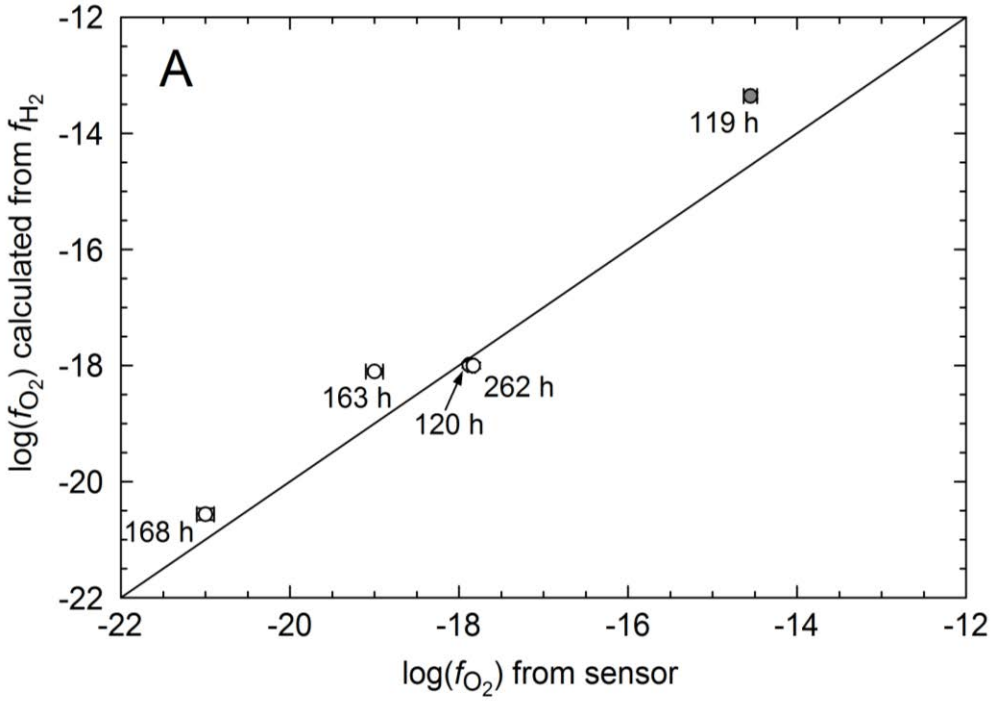

768

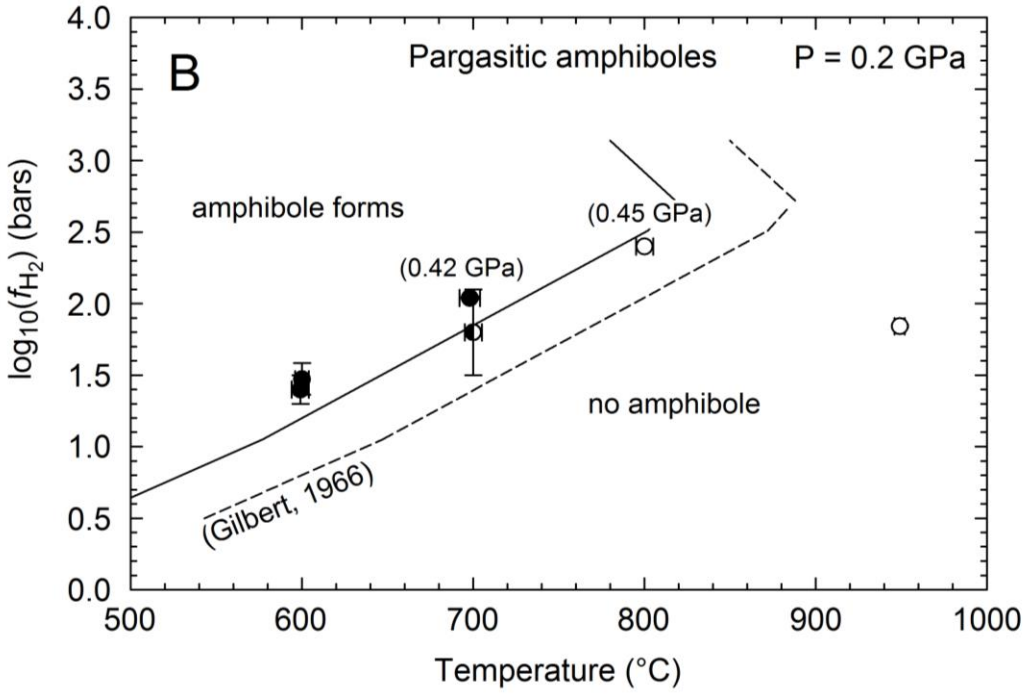

769

770

Always consult and cite the final, published document. See http:/www.minsocam.org or GeoscienceWorld

This is a preprint, the final version is subject to change, of the American Mineralogist (MSA)
Cite as Authors (Year) Title. American Mineralogist, in press.
DOI: https://doi.org/10.2138/am-2019-6768

771 Figure 2

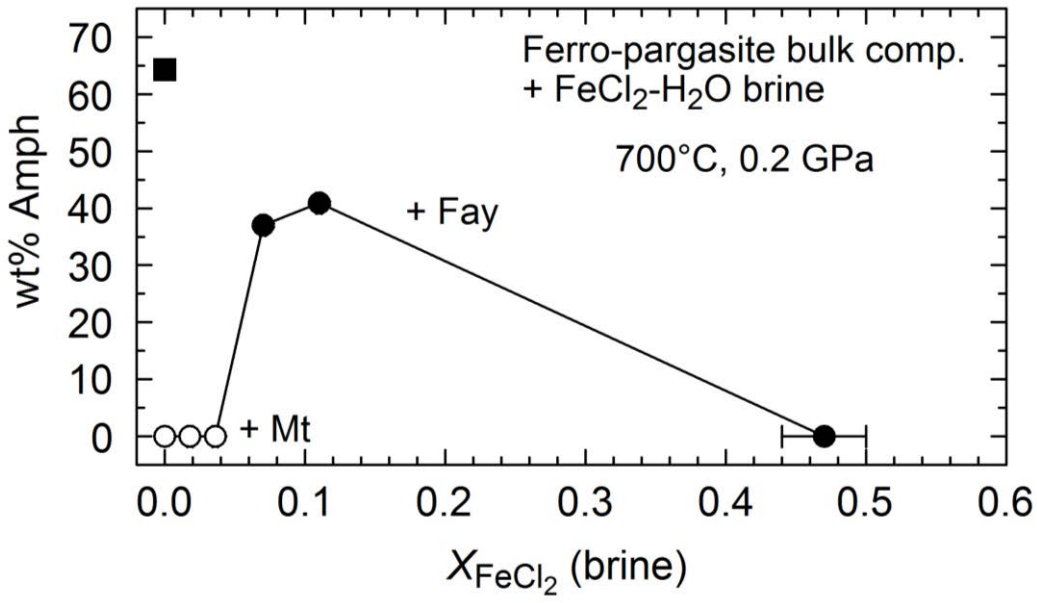

772

773

Always consult and cite the final, published document. See http:/www.minsocam.org or GeoscienceWorld

This is a preprint, the final version is subject to change, of the American Mineralogist (MSA)
Cite as Authors (Year) Title. American Mineralogist, in press.
DOI: https://doi.org/10.2138/am-2019-6768

774 Figure 3a,b

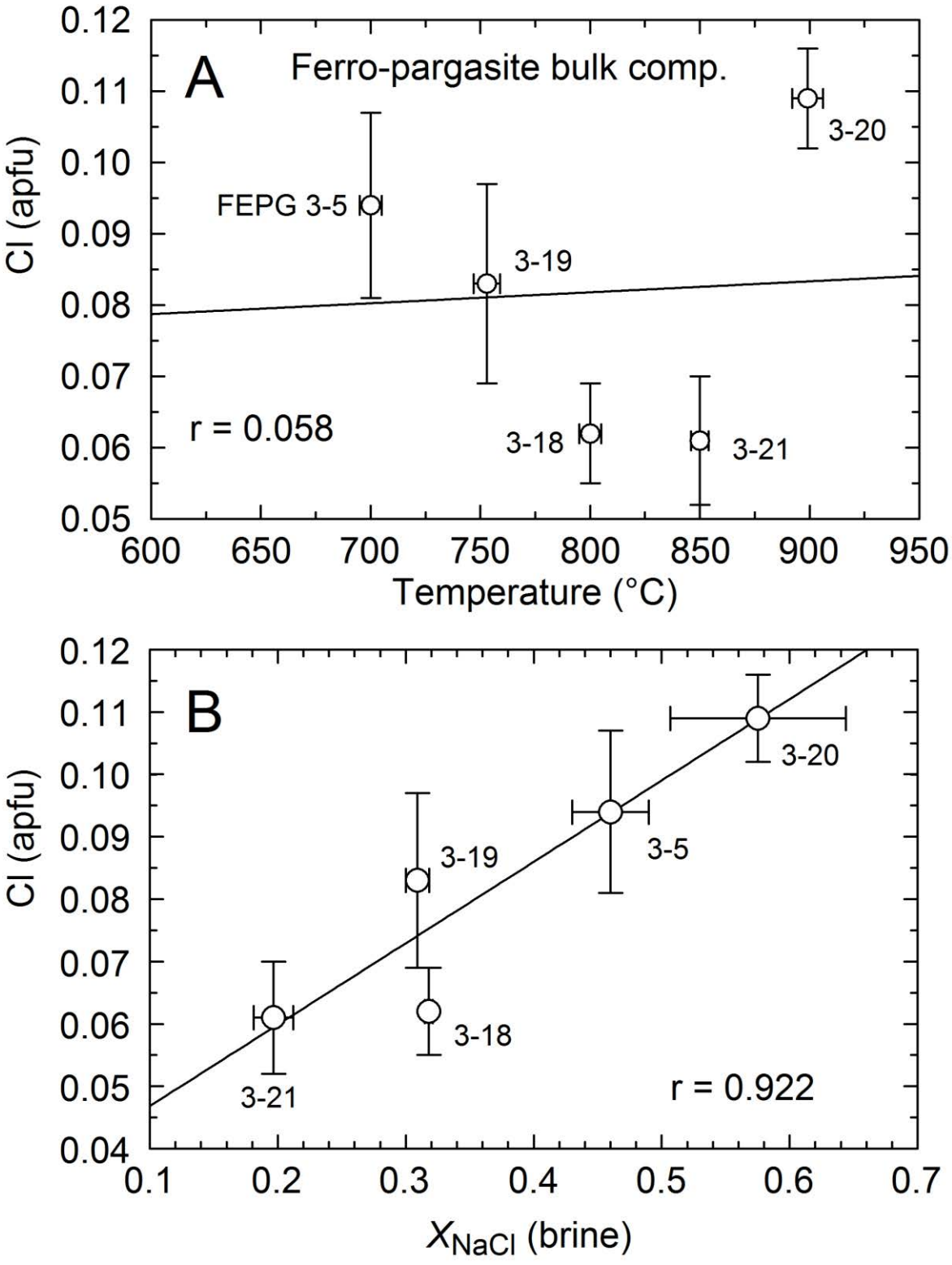

775

776

Always consult and cite the final, published document. See http:/www.minsocam.org or GeoscienceWorld

This is a preprint, the final version is subject to change, of the American Mineralogist (MSA)
Cite as Authors (Year) Title. American Mineralogist, in press.
DOI: https://doi.org/10.2138/am-2019-6768

777 Figure 4

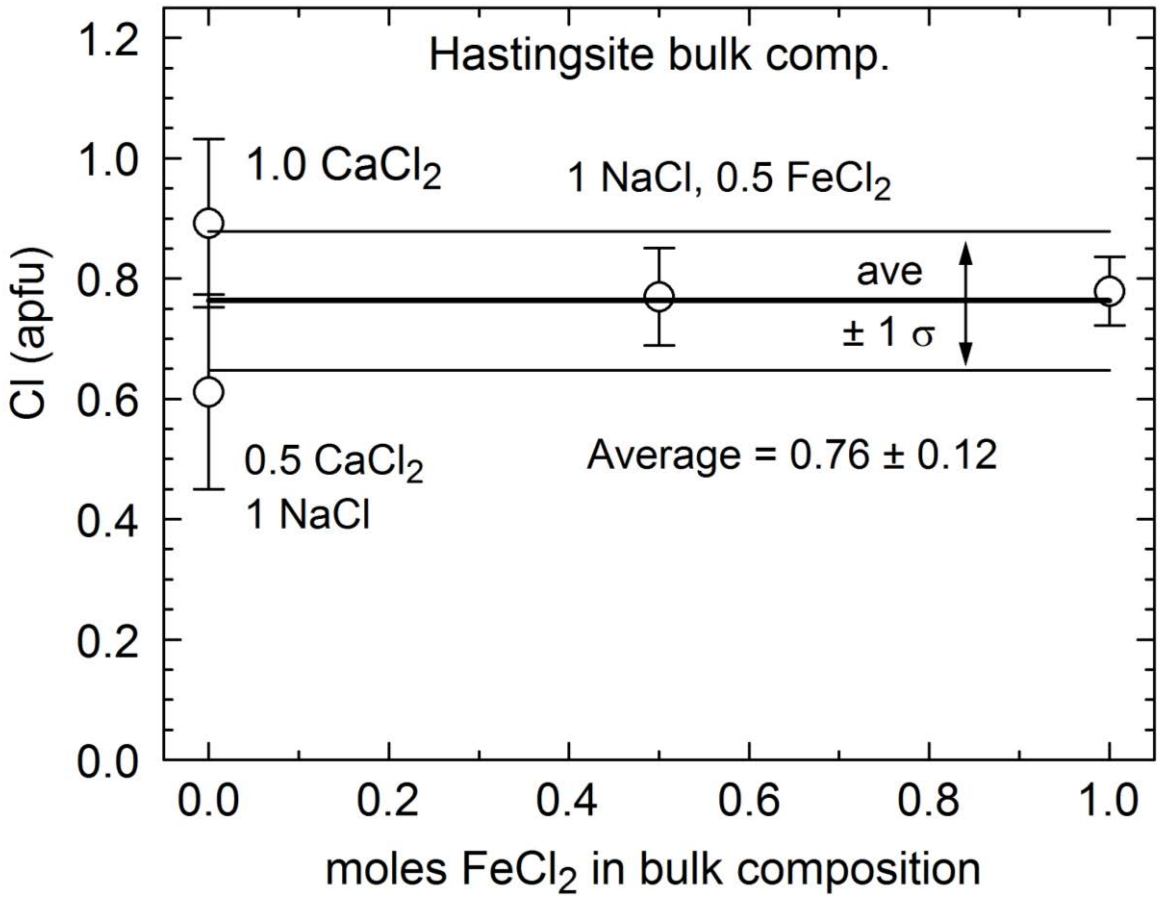

778

779

780

Always consult and cite the final, published document. See http:/www.minsocam.org or GeoscienceWorld

This is a preprint, the final version is subject to change, of the American Mineralogist (MSA)
Cite as Authors (Year) Title. American Mineralogist, in press.
DOI: https://doi.org/10.2138/am-2019-6768

781 Figure 5

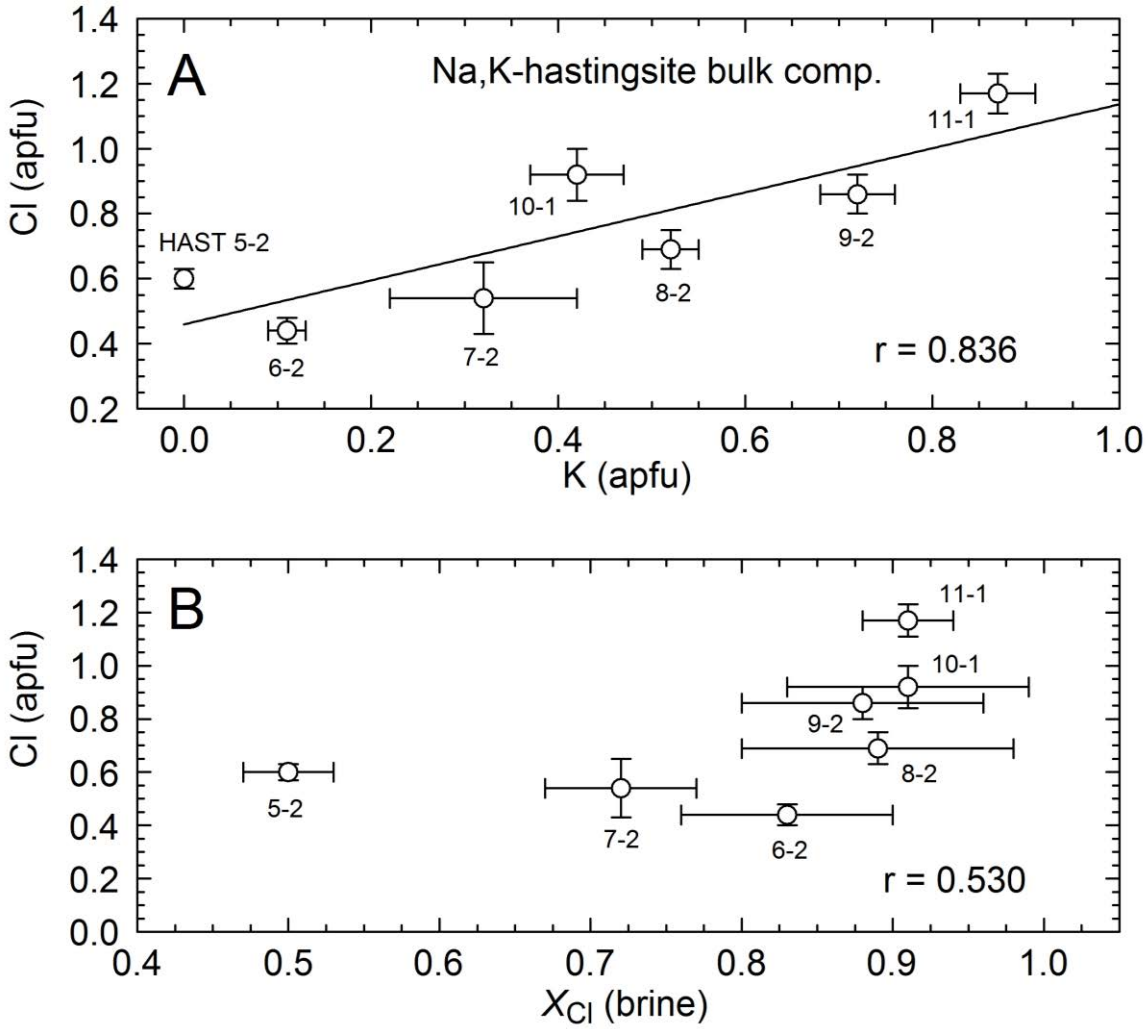

782

783

784

Always consult and cite the final, published document. See http:/www.minsocam.org or GeoscienceWorld

This is a preprint, the final version is subject to change, of the American Mineralogist (MSA)
Cite as Authors (Year) Title. American Mineralogist, in press.
DOI: https://doi.org/10.2138/am-2019-6768

785 Figure 6 a,b

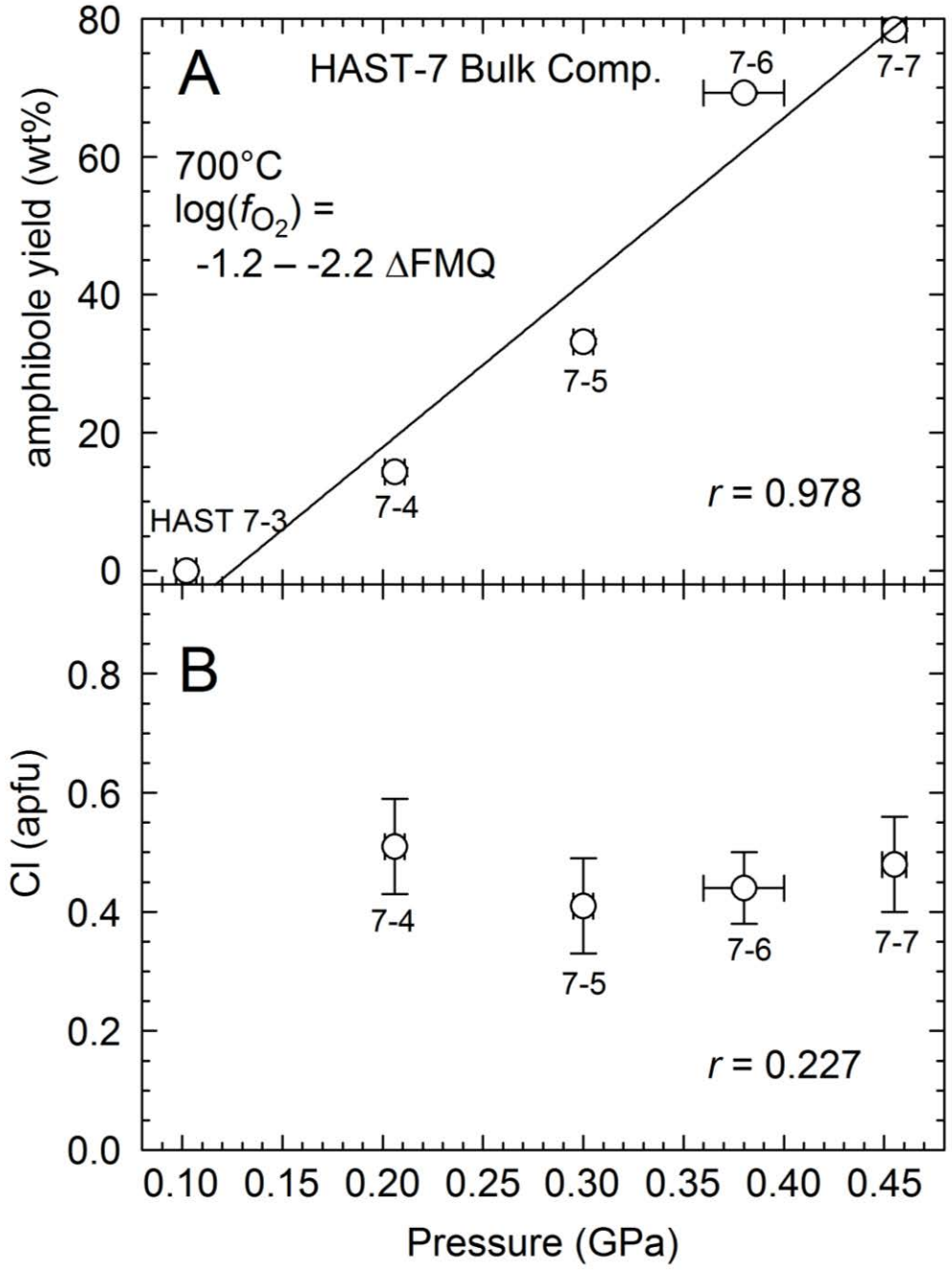

786

787

Always consult and cite the final, published document. See http:/www.minsocam.org or GeoscienceWorld

This is a preprint, the final version is subject to change, of the American Mineralogist (MSA)
Cite as Authors (Year) Title. American Mineralogist, in press.
DOI: https://doi.org/10.2138/am-2019-6768

788 Figure 7

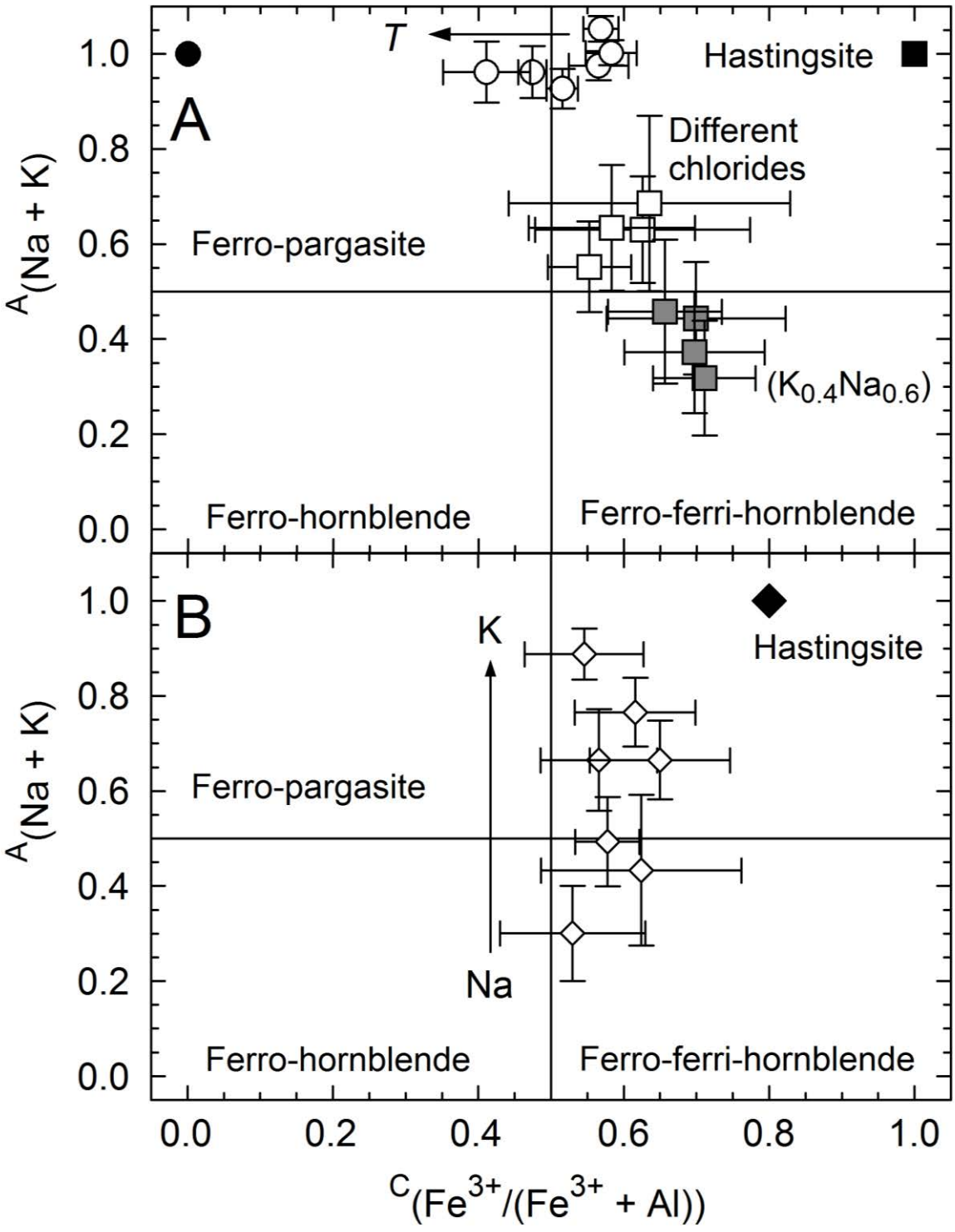

789
790

Always consult and cite the final, published document. See http:/www.minsocam.org or GeoscienceWorld

791 Figure 8

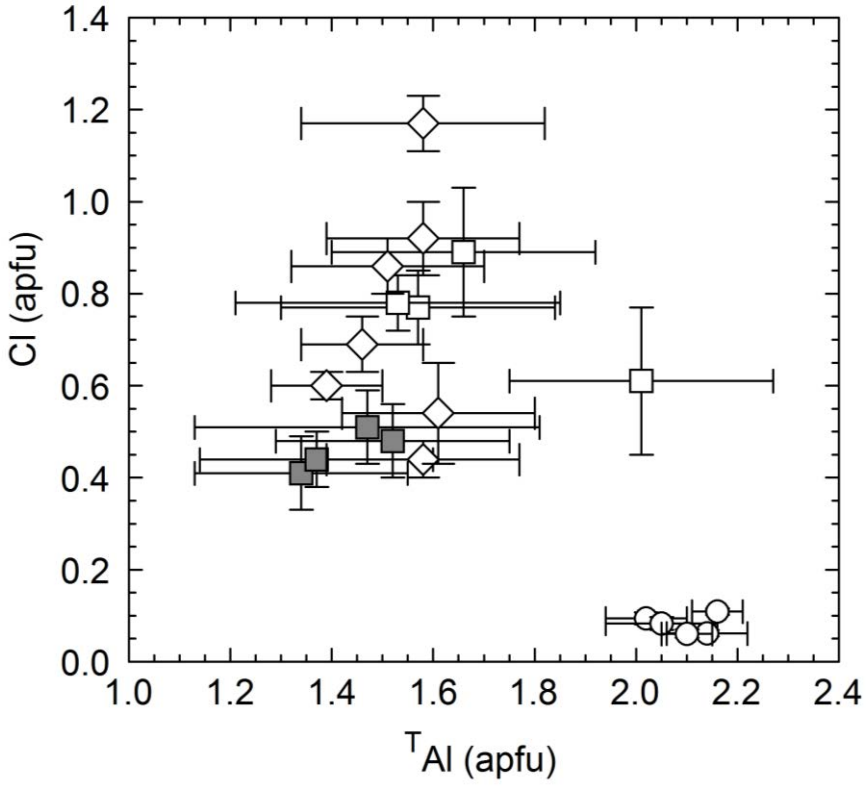

792

793 Figure 9

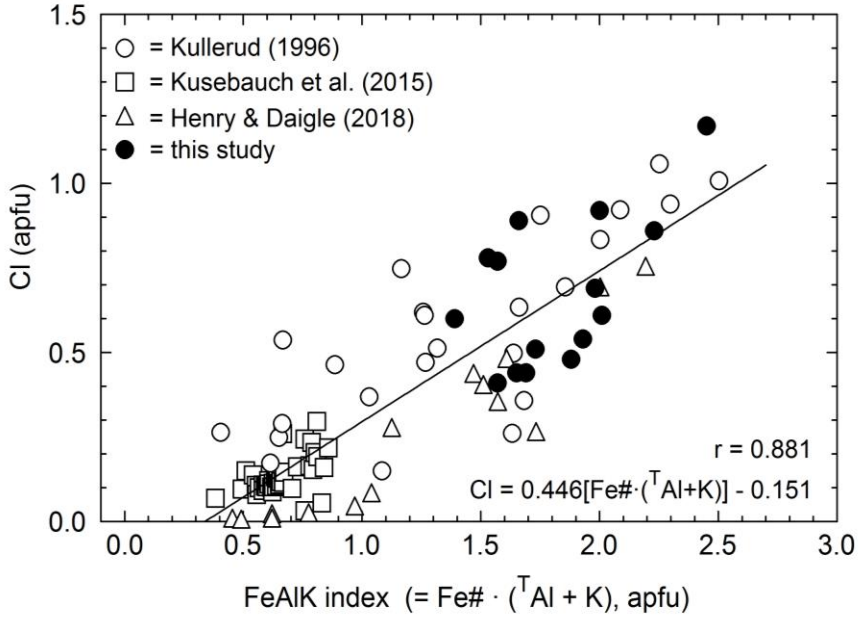

794

Always consult and cite the final, published document. See http:/www.minsocam.org or GeoscienceWorld

This is a preprint, the final version is subject to change, of the American Mineralogist (MSA)
Cite as Authors (Year) Title. American Mineralogist, in press.
DOI: https://doi.org/10.2138/am-2019-6768

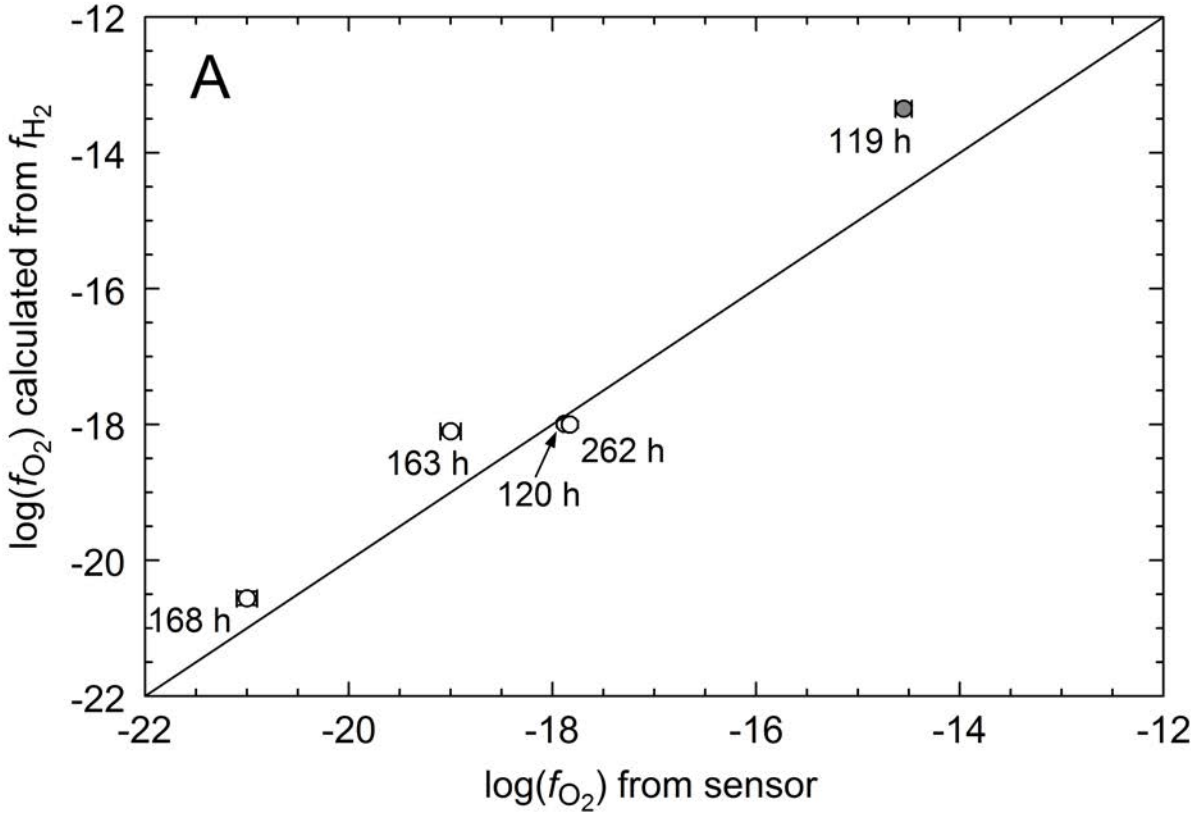

Always consult and cite the final, published document. See http:/www.minsocam.org or GeoscienceWorld

This is a preprint, the final version is subject to change, of the American Mineralogist (MSA)
Cite as Authors (Year) Title. American Mineralogist, in press.
DOI: https://doi.org/10.2138/am-2019-6768

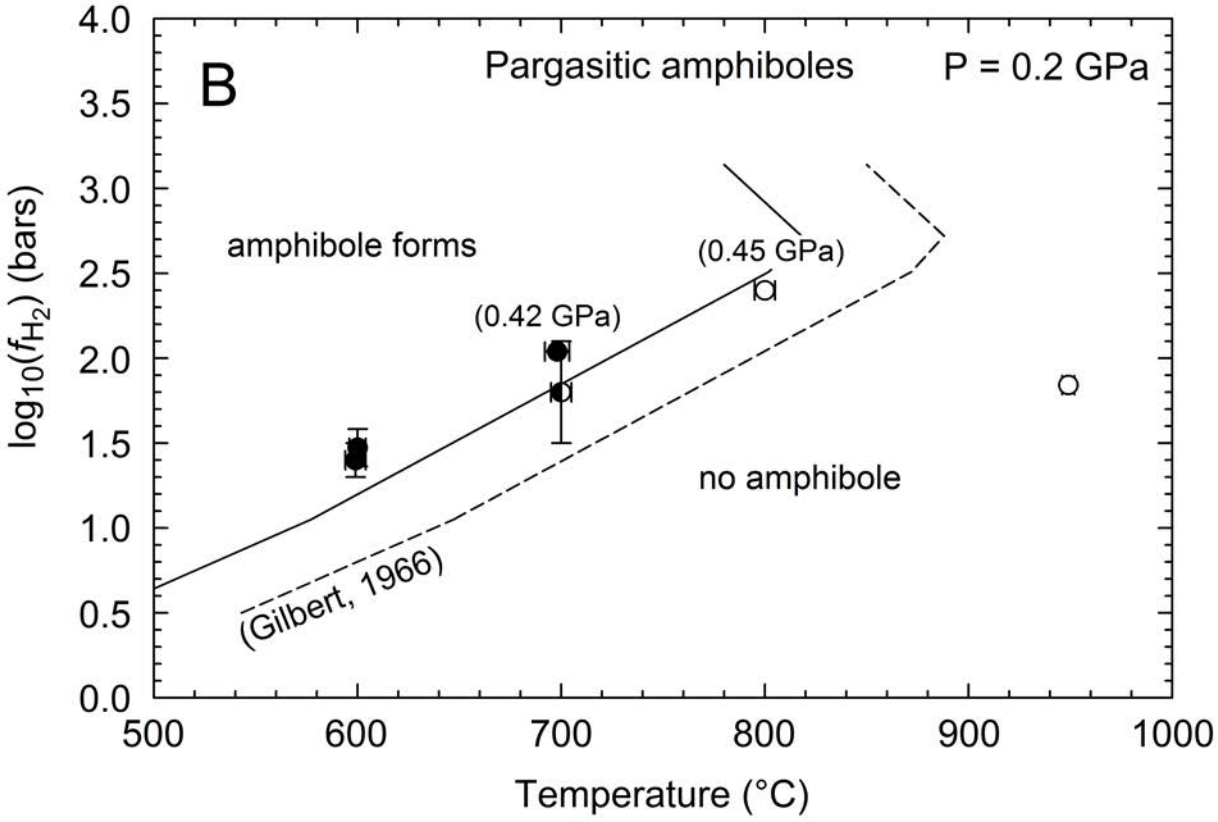

Always consult and cite the final, published document. See http:/www.minsocam.org or GeoscienceWorld

This is a preprint, the final version is subject to change, of the American Mineralogist (MSA)
Cite as Authors (Year) Title. American Mineralogist, in press.
DOI: https://doi.org/10.2138/am-2019-6768

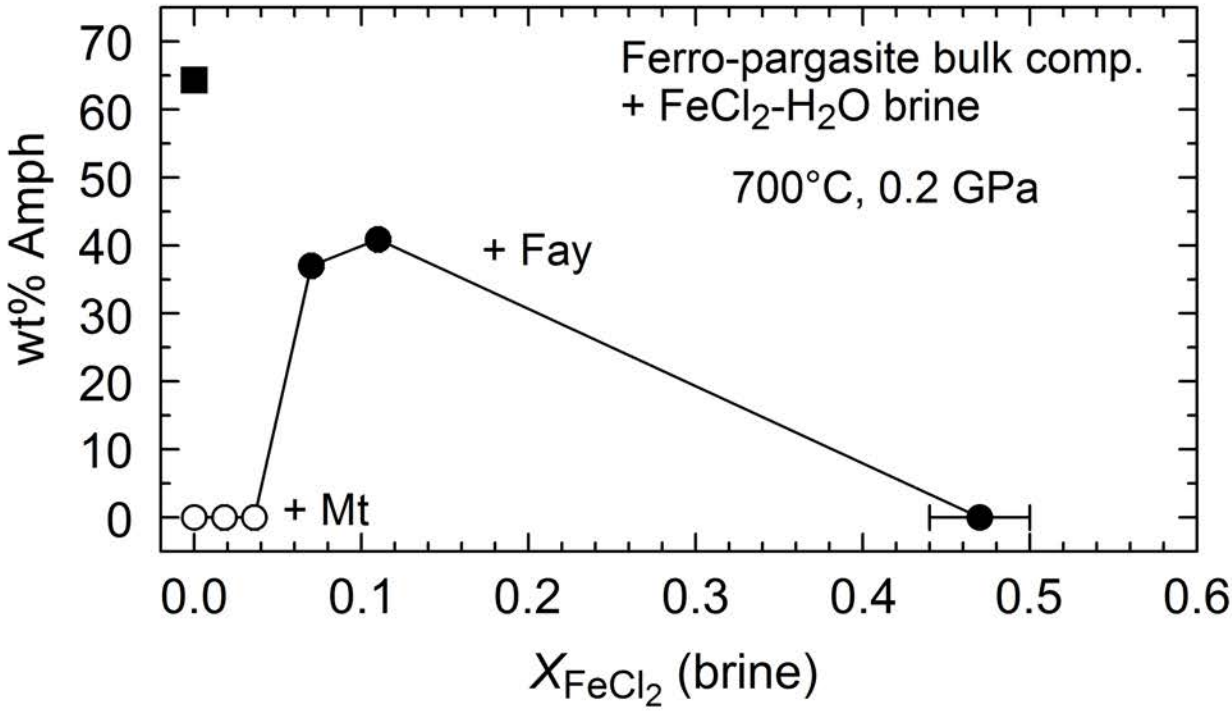

Always consult and cite the final, published document. See http:/www.minsocam.org or GeoscienceWorld

This is a preprint, the final version is subject to change, of the American Mineralogist (MSA)
Cite as Authors (Year) Title. American Mineralogist, in press.
DOI: https://doi.org/10.2138/am-2019-6768

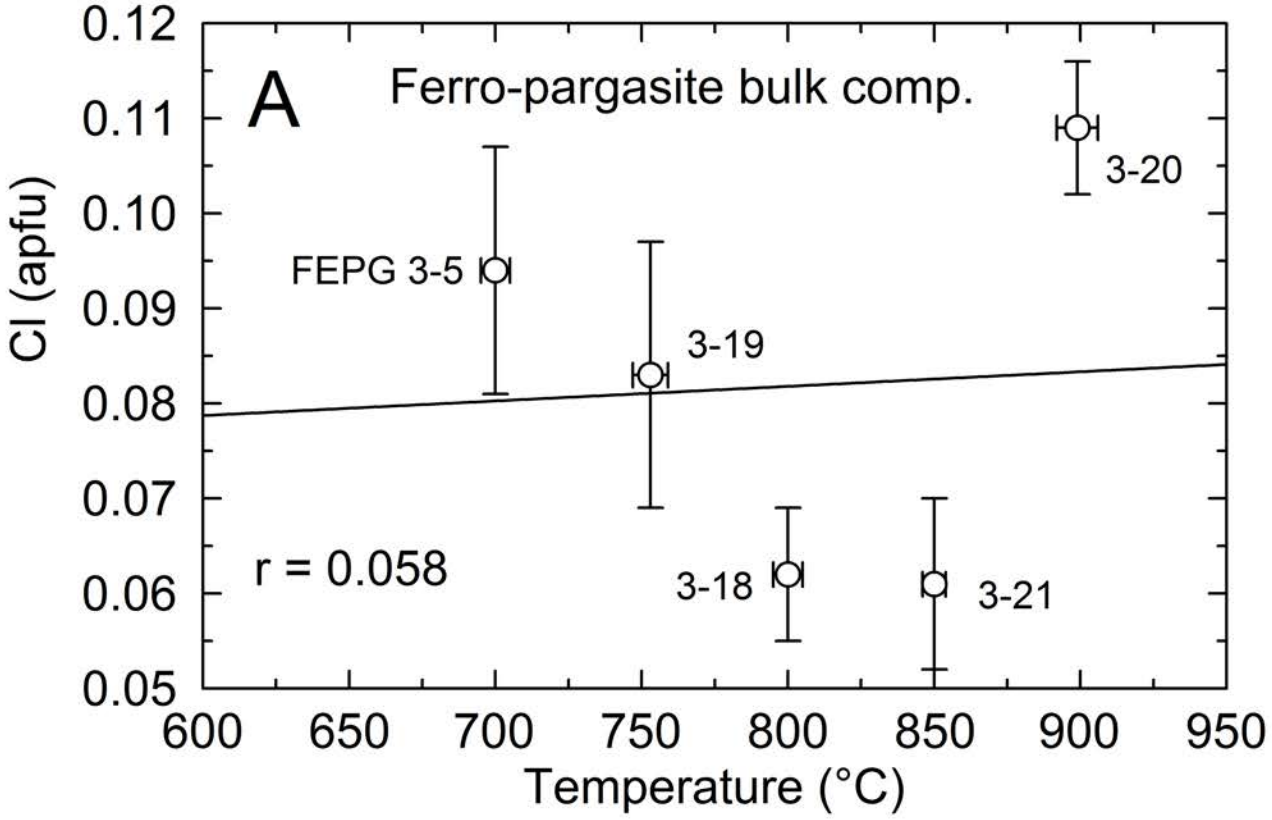

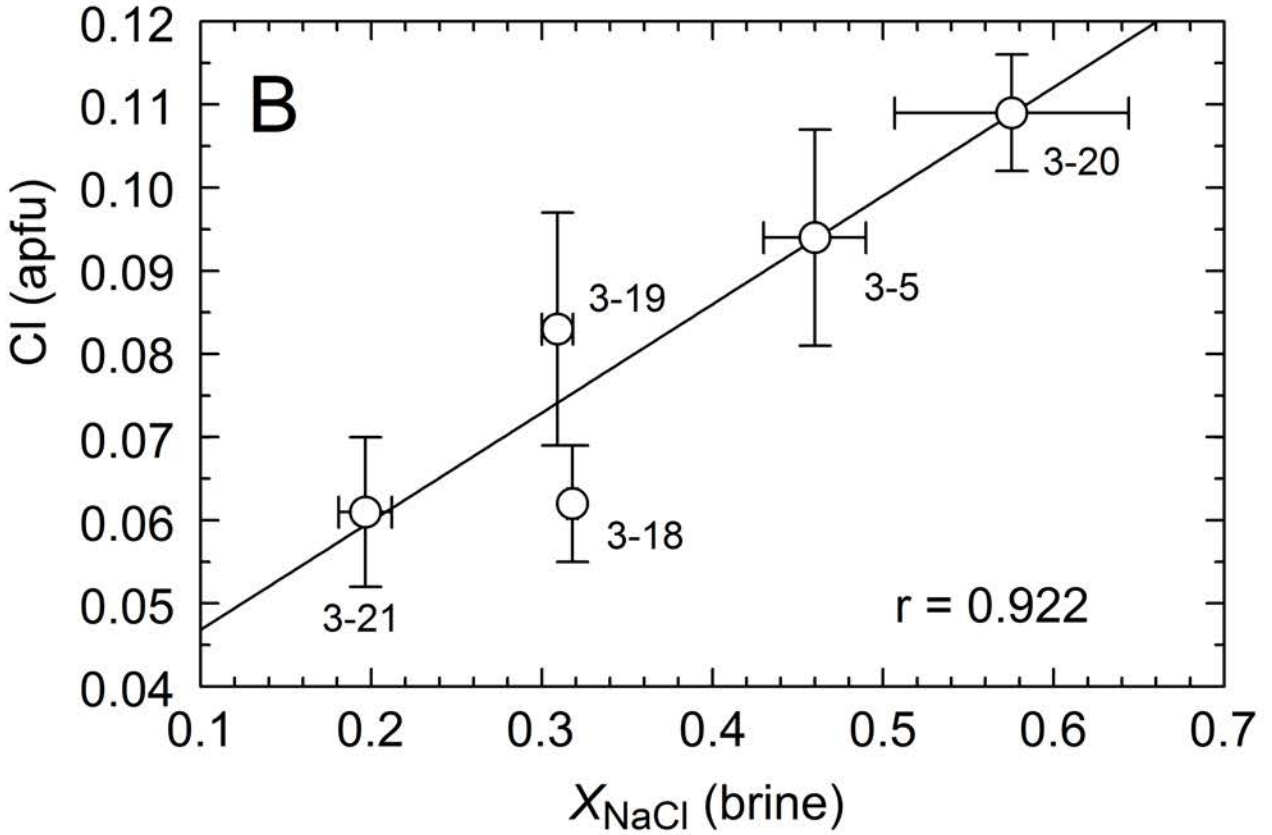

Always consult and cite the final, published document. See http:/www.minsocam.org or GeoscienceWorld

This is a preprint, the final version is subject to change, of the American Mineralogist (MSA)
Cite as Authors (Year) Title. American Mineralogist, in press.
DOI: https://doi.org/10.2138/am-2019-6768

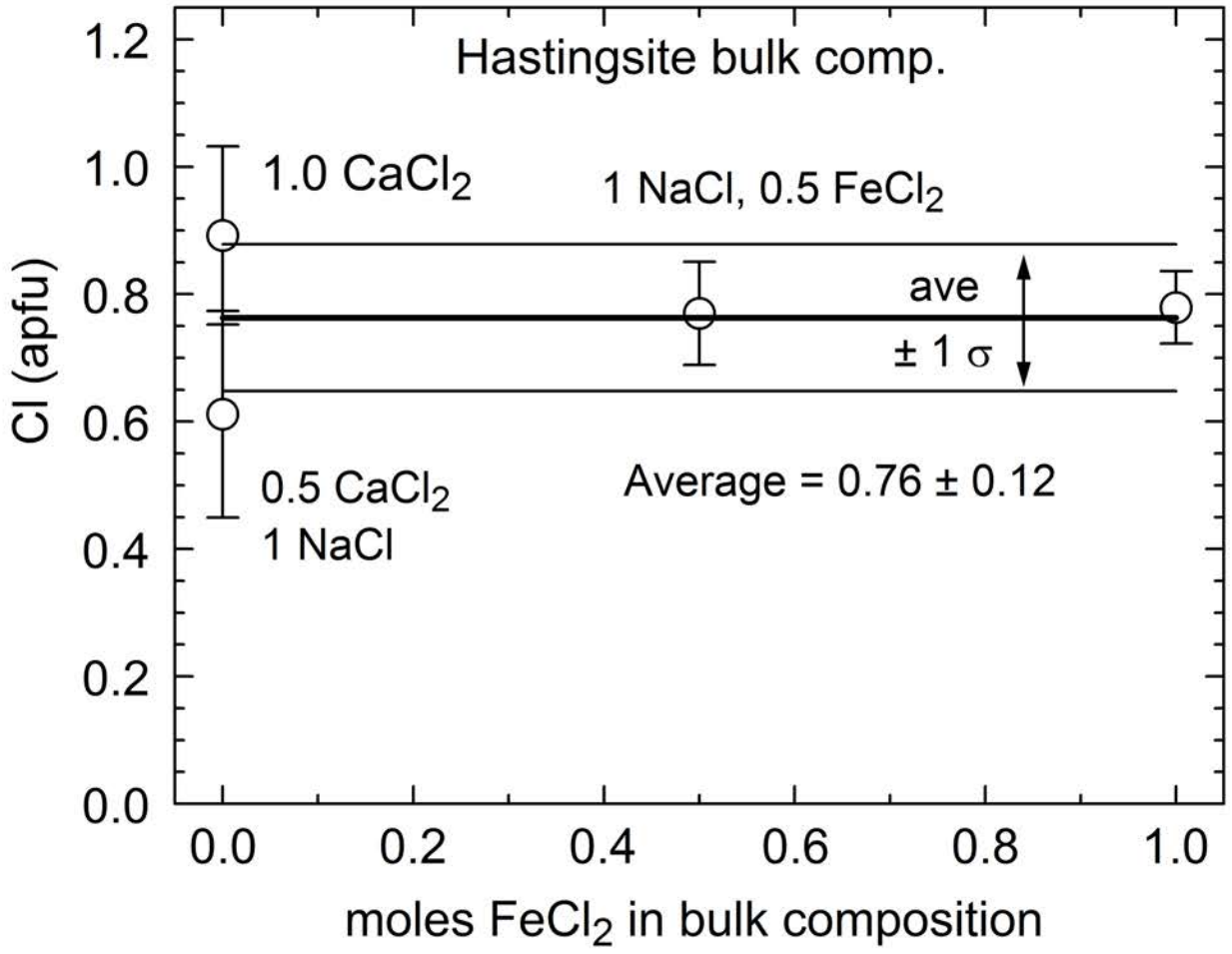

Always consult and cite the final, published document. See http:/www.minsocam.org or GeoscienceWorld

This is a preprint, the final version is subject to change, of the American Mineralogist (MSA)
Cite as Authors (Year) Title. American Mineralogist, in press.
DOI: https://doi.org/10.2138/am-2019-6768

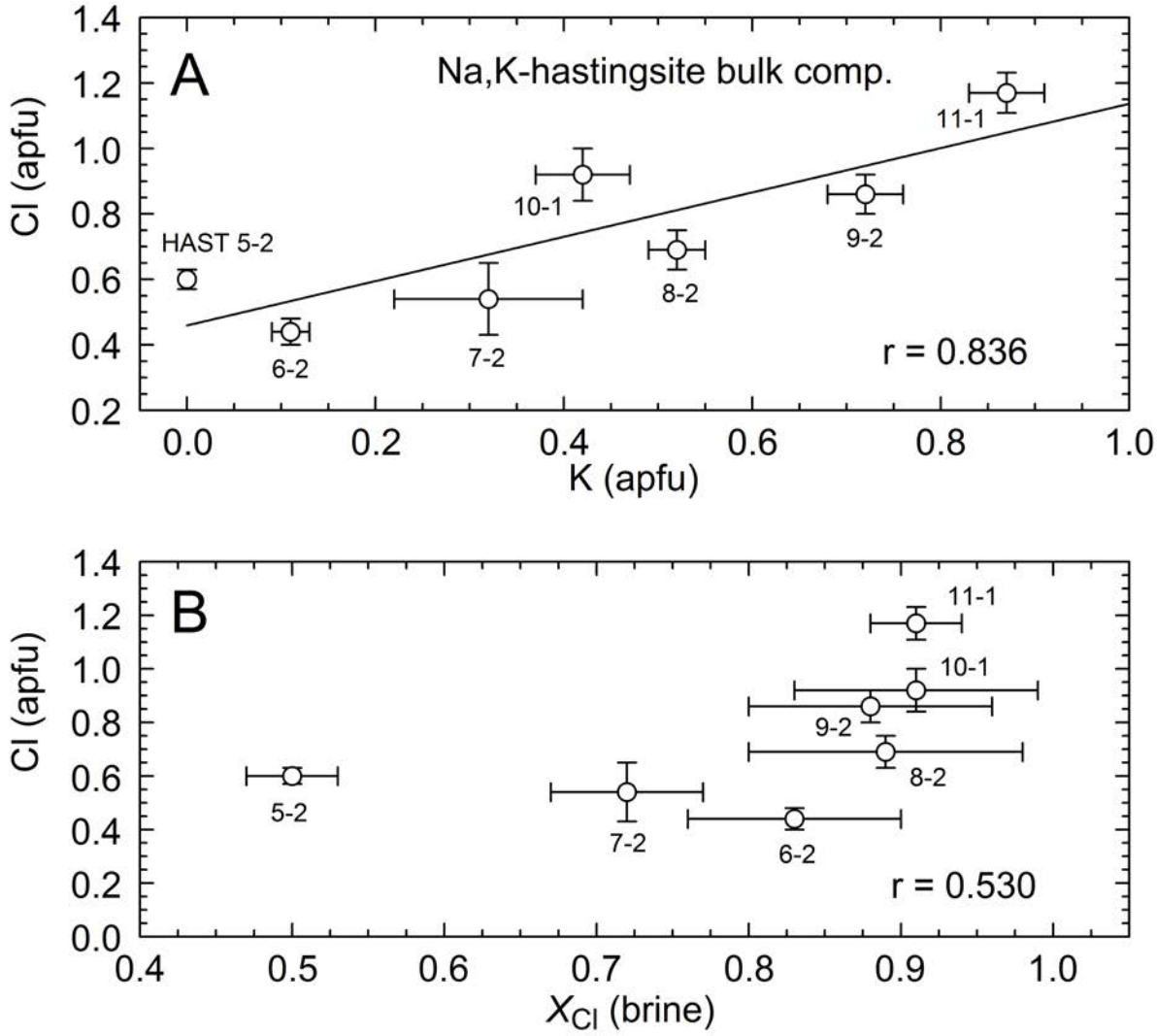

Always consult and cite the final, published document. See http:/www.minsocam.org or GeoscienceWorld

This is a preprint, the final version is subject to change, of the American Mineralogist (MSA)
Cite as Authors (Year) Title. American Mineralogist, in press.
DOI: https://doi.org/10.2138/am-2019-6768

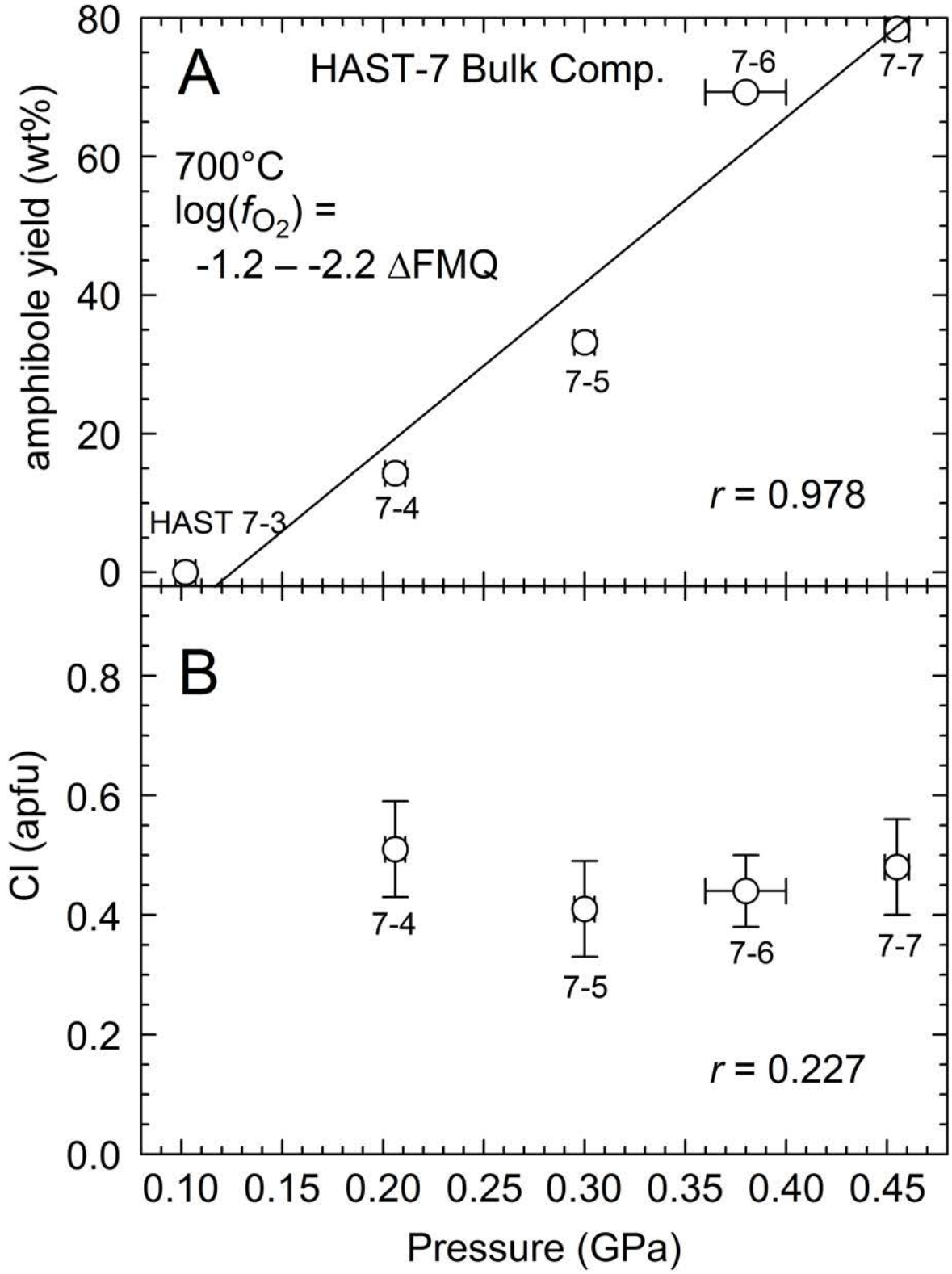

Always consult and cite the final, published document. See http:/www.minsocam.org or GeoscienceWorld

This is a preprint, the final version is subject to change, of the American Mineralogist (MSA)
Cite as Authors (Year) Title. American Mineralogist, in press.
DOI: https://doi.org/10.2138/am-2019-6768

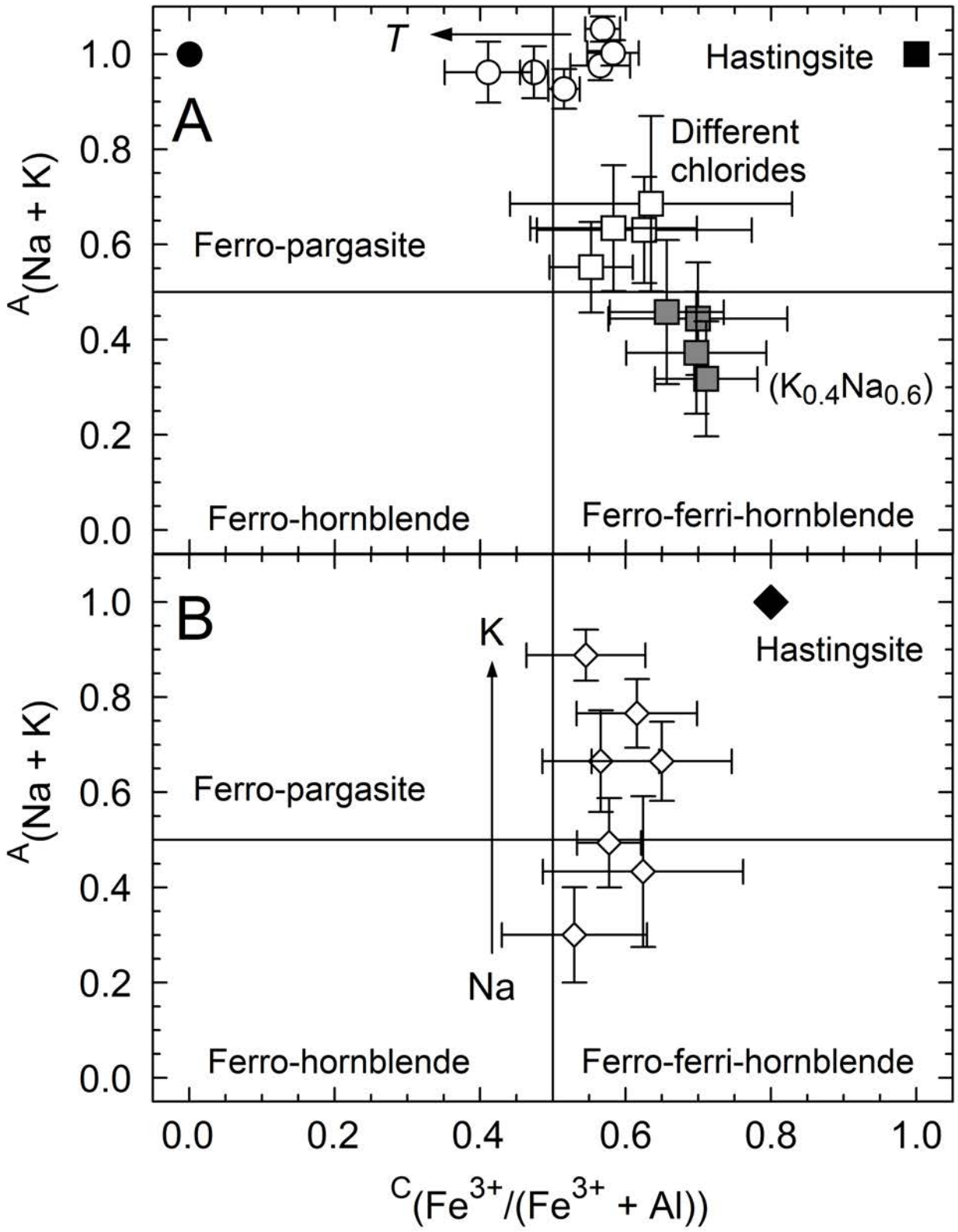

Always consult and cite the final, published document. See http:/www.minsocam.org or GeoscienceWorld

This is a preprint, the final version is subject to change, of the American Mineralogist (MSA)
Cite as Authors (Year) Title. American Mineralogist, in press.
DOI: https://doi.org/10.2138/am-2019-6768

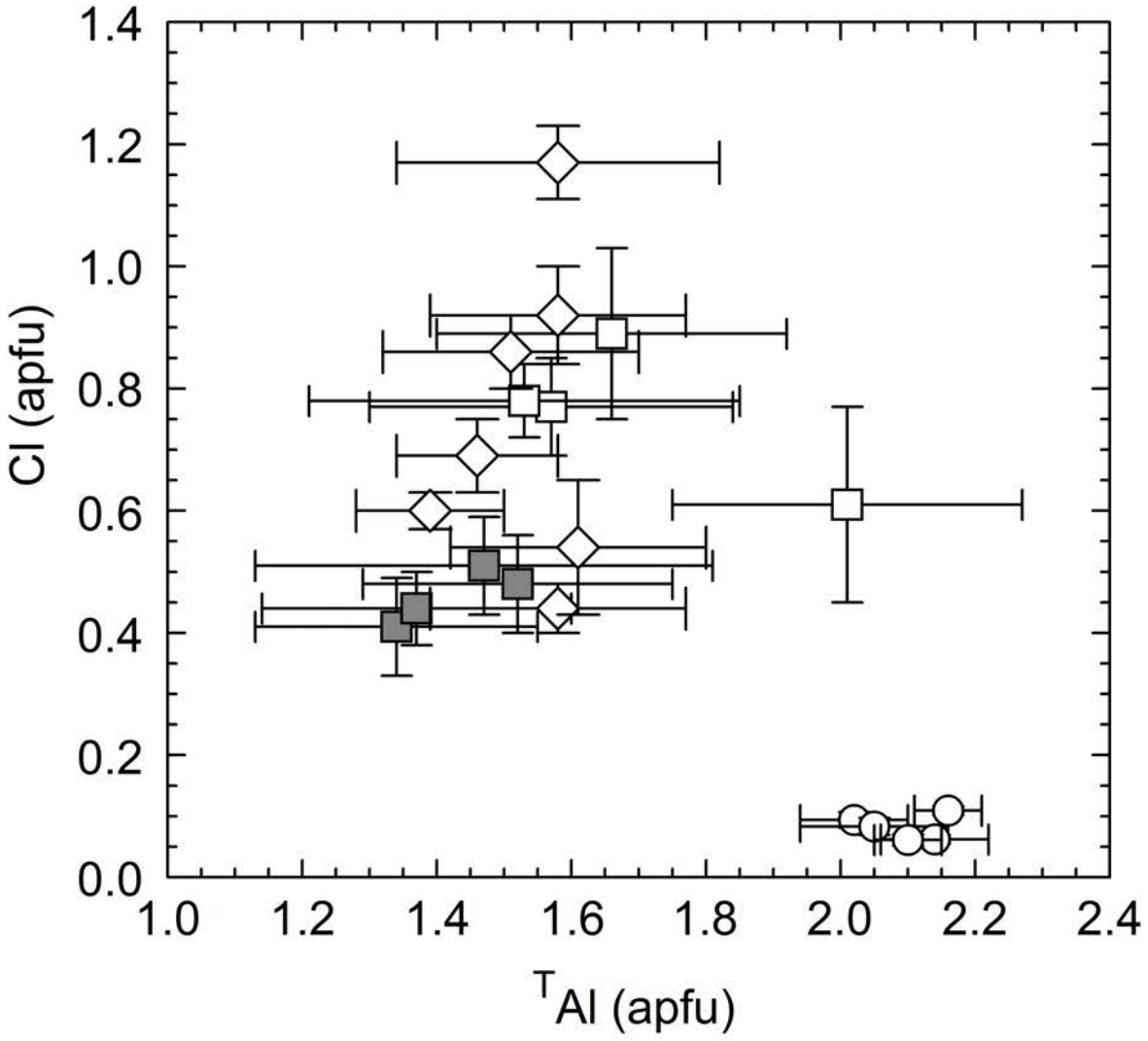

Always consult and cite the final, published document. See http:/www.minsocam.org or GeoscienceWorld

This is a preprint, the final version is subject to change, of the American Mineralogist (MSA)
Cite as Authors (Year) Title. American Mineralogist, in press.
DOI: https://doi.org/10.2138/am-2019-6768

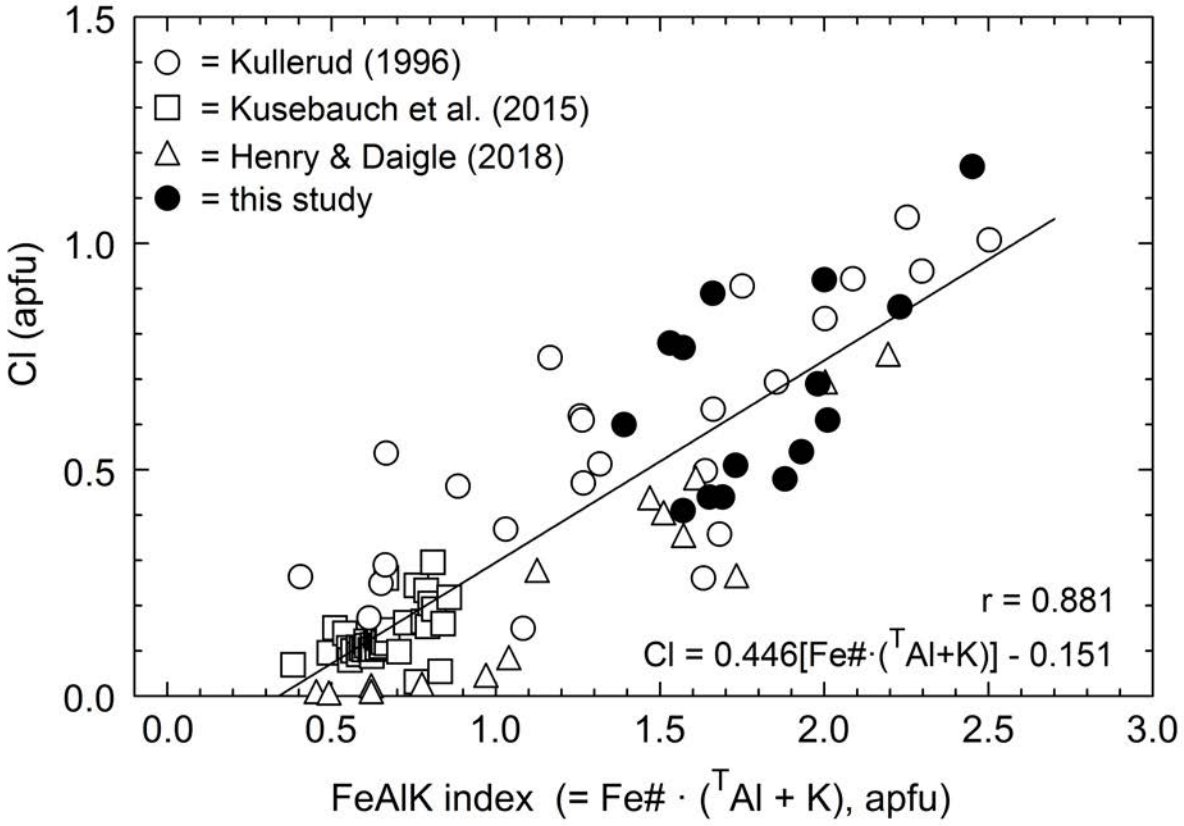

Always consult and cite the final, published document. See http:/www.minsocam.org or GeoscienceWorld